GABA$_A$ and serotonergic receptors participation in anxiolytic effect of chalcones in adult zebrafish

Francisco Rogênio Silva Mendes, Antonio Wlisses da Silva, Maria Kueirislene Amâncio Ferreira, Emanuela de Lima Rebouças, Italo Moura Barbosa, Matheus Nunes da Rocha, Walber Henrique Ferreira Ribeiro, Ramon Róseo Paula Pessoa Bezerra de Menezes, Emanuel Paula Magalhães, Emanuelle Machado Marinho, Márcia Machado Marinho, Paulo Nogueira Bandeira, Jane Eire Silva Alencar de Menezes, Emmanuel Silva Marinho & Hélcio Silva dos Santos

　　📄 View supplementary material ⧉

　　📅 Published online: 16 Jan 2023.

　　✏️ Submit your article to this journal ⧉

　　🔍 View related articles ⧉

　　CrossMark View Crossmark data ⧉

Taylor & Francis
Taylor & Francis Group

Check for updates

GABAA and serotonergic receptors participation in anxiolytic effect of chalcones in adult zebrafish

Francisco Rogênio Silva Mendes[a] (iD), Antonio Wlisses da Silva[b] (iD), Maria Kueirislene Amâncio Ferreira[c] (iD), Emanuela de Lima Rebouças[b] (iD), Italo Moura Barbosa[c] (iD), Matheus Nunes da Rocha[d] (iD), Walber Henrique Ferreira Ribeiro[e], Ramon Róseo Paula Pessoa Bezerra de Menezes[f] (iD), Emanuel Paula Magalhães[f] (iD), Emanuelle Machado Marinho[g] (iD), Márcia Machado Marinho[a] (iD), Paulo Nogueira Bandeira[e] (iD), Jane Eire Silva Alencar de Menezes[c] (iD), Emmanuel Silva Marinho[c,d] (iD) and Hélcio Silva dos Santos[a,b,e] (iD)

[a]Department of Biological Chemistry, Regional University of Cariri, Crato, Ceará, Brazil; [b]Graduate Program of Biotechnology, State University of Ceara, Fortaleza, Ceará, Brazil; [c]Graduate Program in Natural Sciences, State University of Ceara, Fortaleza, Ceará, Brazil; [d]Department of Chemistry, Limoeiro do Norte, State University of Ceara, Limoeiro do Norte, Ceará, Brazil; [e]Chemistry Course, State University of Vale do Acaraú, Sobral, Ceará, Brazil; [f]Department of Clinical and Toxicological Analysis, Federal University of Ceará, Fortaleza, Ceará, Brazil; [g]Department of Analytical and Physical Chemistry, Federal University of Ceara, Fortaleza, Ceará, Brazil

Communicated by Ramaswamy H. Sarma

ABSTRACT

The prevalence of anxiety is a significant public health problem, being the 24th leading cause of disability in individuals affected by this disorder. In this context, chalcones, a flavonoid subclass obtained from natural or synthetic sources, interact with central nervous system (CNS) receptors at the same binding site as benzodiazepines, the primary drugs used in the treatment of anxiety. Thus, our study investigates the anxiolytic effect of synthetic chalcones derived from the natural product 2-hydroxy-3,4,6-trimethoxyacetophenone isolated from *Croton anisodontus* Müll.Arg. in modulating anxiolytic activity via GABAergic and serotoninergic neurotransmission in an adult zebrafish model. Chalcones 1 and 2 were non-toxic to adult zebrafish and showed anxiolytic activity via GABAA receptors. Chalcone 2 also had its anxiolytic action reversed by the antagonist granisetron, indicating the participation of serotonergic receptors 5HTR3A/3B in the anxiolytic effect. In addition, molecular docking results showed that chalcones have a higher affinity for the GABAA receptor than DZP and binding in the same region of the DZP binding site, indicating a similar effect to the drug. Furthermore, the interaction of chalcones with GABAA and 5-HT3A receptors demonstrates the anxiolytic effect potential of these molecules.

1. Introduction

Anxiety-related mental health problems are estimated at 3.6% globally, 4.2% in the UK and 6.3% in the US (World Health Organization, 2017). Anxiety is a major public health problem (Chisholm et al., 2016). In 2019 alone, anxiety was the 24th leading cause of disability (Vos et al., 2020). However, mental health should not be seen as something that resides solely in the individual but rather as systems, e.g., mental health systems, political systems and education systems, and all contribute to mental health at the individual, community and societal levels (Hanson & Gottesman, 2012).

Endogenous serotonergic, gamma-aminobutyric acid (GABAA) receptor A and opioid systems are critical for regulating many physiological and behavioral functions. For example, in anxiety, GABAA receptors can be allosterically modulated by drugs such as benzodiazepines (BDZs), causing anxiolytic effects (Marder, 2012). Within the seven significant classes of 5-HT (serotonin) receptors, the 5-HT1A subtype plays an essential role in regulating mental disorders such as depression, anxiety or schizophrenia (Celada et al., 2013).

Benzodiazepines are the class of drugs indicated for the treatment of anxiety, including lorazepam and diazepam. However, concerns have been raised about the short- and long-term risks associated with BZDs (Ferreira et al., 2021). They act on the Central Nervous System (CNS) through the neurotransmitter gamma-aminobutyric acid (GABA), the primary inhibitory neurotransmitter in the brain, and bind to GABAA receptors, where they potentiate the inhibitory action of GABA (Buxeraud & Faure, 2019).

Despite anxiolytic and antidepressant drugs, there is a need to develop more effective pharmacotherapies with fewer side effects than existing drugs (Higgs et al., 2019). The first natural chalcones were isolated in 1910 and occur mainly as pigments responsible for the coloration of the petals of flowers, leaves, bark, fruits and roots of various plants (Salehi et al., 2021).

The flavonoid subclass chalcones are benzyl acetophenones, α, β-unsaturated ketones containing two aromatic rings (A and B) with different substituents. In chalcones, the two aromatic rings are connected by an aliphatic three-carbon series (Rojas et al., 2002). Natural and synthetic derivatives of chalcone have shown promising biological activity as an antioxidant, anti-inflammatory, anti-cancer, and anti-infective agent (De Campos-Buzzi et al., 2007; Higgs et al., 2019). This class of compounds has shown therapeutic potential mainly due to interactions with GABA$_A$ receptors (Silva Mendes et al., 2022) and the serotonergic system (Ferreira et al., 2020). In the zebrafish model, chalcones have shown anxiolytic and anticonvulsant effects (Maria Kueirislene Amâncio Ferreira et al., 2021).

This study investigated the anxiolytic effect of synthetic chalcones derived from the natural product 2-hydroxy-3,4,6-trimethoxyacetophenone isolated from *Croton anisodontus* Müll.Arg. in the modulation of anxiolytic activity via GABAergic and serotoninergic neurotransmission in an adult zebrafish model, as well as the structure-activity relationship and the importance of electron-withdrawing groups in different positions of the B ring of chalcones and their interactions with biological receptors of the central nervous system.

2. Materials and methods

2.1. Drugs and reagents

Drugs/reagents used were Granisetron hydrochloride (Corepharma, Middlesex, NJ, USA), pizotifene maleate (Central Manipulation Pharmacy, São Paulo, SP, Brazil), fluoxetine (Eli Lilly, Indianapolis, IN, USA), cyproheptadine (Evidence Pharmaceutical Solutions, Fortaleza, CE, Brazil), DZP, and PTZ (Sigma-Aldrich, Missouri, USA). Flumazenil was purchased from Roche Pharmaceutical (Welwyn Garden City, UK).

2.2. Synthesis and chemical characterization of chalcones

A description of the procedure for the synthesis of chalcones **1** and **2** is shown in Scheme 1 was synthesized using a Claisen–Schmidt condensation reaction in a primary medium. An ethanol solution of 2-hydroxy-3,4,6-trimethoxyacetophenone isolated from *Croton anisodontus* (Scheme 1) (2 mmol) was added to a solution of 3-nitrobenzaldehyde and 4-nitrobenzaldehyde (2 mmol), followed by the addition of 10 drops of 50% w/v aqueous NaOH and stirred for 48 h at room temperature 32 °C (da Silva et al., 2020). Chalcones ware then filtered under reduced pressure, washed with cold water, dried, and recrystallized from ethanol, and then purity

(99.9%) was checked by HPLC analysis (Figure S1, Supplementary material). The structure of the heterocyclic chalcone was in agreement with the literature (da Silva et al., 2020) and is confirmed by analyzing ^{1}H, ^{13}C, and infrared spectra (Figures S1–S4, Supplementary material), which were obtained using a Bruker DPX-300 platform operating at frequencies of 300 MHz for hydrogen and 75 MHz for carbon. In addition, the infrared absorption spectrum was obtained using a Bruker vacuum spectrometer (VERTEX 70 V) with a HeNe laser source with a wavelength of 633 nm. Finally, the chromatographic evaluation was performed by HPLC (Agilent 1260 Infinity, Germany) equipped with a C-18 reverse phase column (Agilent Eclipse Plus: 3.5 μm, 4.6 × 100 mm).

2.3. Zebrafish

Zebrafish (*Danio rerio*) (age 90 to 120 days; 0.4 ± 0.1 g, 3.5 ± 0.5 cm) of both sexes were purchased from a local store (Fortaleza, CE). The animals were kept in a 10-L glass aquarium (30 × 15 × 20 cm) at a temperature of 25 ± 2 °C, in 10–14 h (light/dark) cycles, with dechlorinated water (pH 7.0, ProtecPlus®) using an air pump with submerged filters. Fish were fed (Spirulina®) 24 h before experiments. Before each treatment, animals were anesthetized in iced water, and following experiments, they were euthanized by immersion in iced water (0-3 °C) for 1 min or until loss of opercular movements. This study was approved by the Ethics Committee on the Use of Animals at the State University of Ceará (CEUA-UECE; no. 04983945/2021), in accordance with ethical principles involving animal experiments.

2.4. Acute toxicity assay

A 96-h acute toxicity assessment was performed using adult zebrafish according to the guidelines of the Organization for Economic Cooperation and Development (OECD) (Amali et al., 2019). Animals (n = 6/group) were treated orally (20 μL) with chalcones **1** and **2** (1.0, 3.0 or 10 mg/kg) or vehicle (Control; DMSO 3%). After treatment, the animals were left to rest to analyze mortality rates. From 24 h to 96 h, the number of dead fish in each group was recorded, and the lethal dose capable of killing 50% of the animals (LD50) was determined using the mathematical method trimmed Spearman-Karber with 95% confidence intervals (Arellano-Aguiar et al., 2015).

2.5. Open-field test

To assess changes in the animals' motor coordination, an open field test was performed (Ahmad & Richardson, 2013). Initially, the fish (n = 6/group) were treated orally (*p.o.*) with chalcones 1
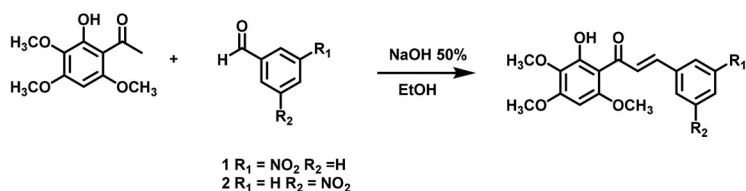
Scheme 1. Synthesis of chalcones **1** and **2**.

and 2 at doses of 1.0, 3.0, 10 mg/kg, DZP (10 mg/kg), or vehicle (Control; 3% DMSO). A group of untreated animals was included (naive group). After 1 h of treatment, animals were added to glass Petri dishes (10 × 15 cm) containing the same aquarium water, marked with four quadrants, and analyzed for locomotor activity by counting the number of crossing lines (CL) by the animals (Gonçalves et al., 2020).

2.6. Anxiolytic activity

Animal anxiety behavior was observed using a light/dark test. Similar to rodents, zebrafish naturally avoid lighted areas (Gonçalves et al., 2020). The experiment was carried out in a glass aquarium (30 cm × 15 cm × 20 cm) divided into light and dark areas. The aquarium was filled with chlorine-free tap water, which simulated a new shallow environment different from the conventional aquarium and capable of inducing anxiety behaviors. In animals (n = 6/group), 20 μL of chalcones **1** and **2** ware administered orally at doses of 0,5; 1.0; 3.0 and 10 mg/kg. Negative and positive control groups consisted of 3% DMSO and 10 mg/kg DZP solution, respectively. An untreated group (naive) was also included. After 1 h, animals were individually placed in the clear zone, and the anxiolytic effect was measured based on the time spent in the clear zone of the aquarium within 5 min of observation (Gebauer et al., 2011).

2.7. Evaluation of GABAergic and serotoninergic neuromodulation

The mechanisms of action involved in the anxiolytic-like effect of chalcones **1** and **2** were identified through pretreatment with flumazenil (a neutralizing modulator of positive modulators) and serotonergic antagonists cyproheptadine (5-HTR$_{2A}$ antagonist), pizotifen (5-HTR$_1$ and 5-HTR$_{2A/2C}$ antagonist), and granisetron (5-HTR$_{3A/3B}$ antagonist) before the light/dark test (Benneh et al., 2017). Zebrafish (n = 6/group) were pretreated with flumazenil (4 mg/kg; 20 μL; p.o.), cyproheptadine (32 mg/kg; 20 μL; p.o.), pizotifen (32 mg/kg; 20 μL; p.o.), or granisetron (20 mg/kg; 20 μL; p.o.). After 15 min, the highest effective dose of chalcones **1** and **2** (10 mg/kg; 20 μL; p.o.) found in the pilot test was administered (see the previous section); 3% DMSO (vehicle; 20 μL; p.o.) was used as a negative control. DZP (10 mg/kg, 20 μL; p.o.) and fluoxetine (0.05 mg/kg; i.p.) were used as GABA$_A$ and 5-HT agonists, respectively. After 1 h of treatment, animals were subjected to the light/dark test as described in the previous section.

2.8. Molecular docking methodology

2.8.1. Computational details

To carry out the simulations, the codes used were: MarvinSketch[TM] 19.12.0 (http://www.chemaxon.com) (Csizmadia, 2019), Avogadro[TM] (http://avogadro.cc/) (Hanwell et al., 2012), Autodocktools[TM] (Huey et al., 2012), AutoDockVina[TM] (Trott & Olson, 2010), UCSF Chimera[TM] (Pettersen et al., 2004), Discovery studio visualizer[TM] viewer (Biovia, 2016) and Pymol (DeLano, 2020).
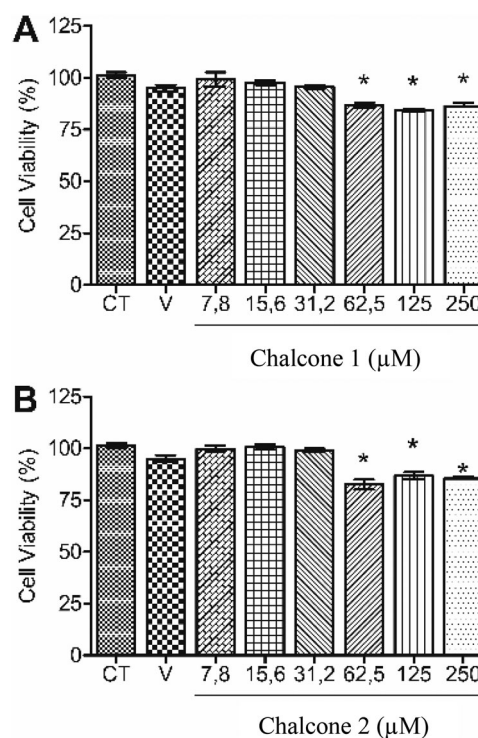
Figure 1. Cytotoxicity of chalcone 1 (A) and chalcone 2 (B) on PC12 cells by MTT assay. Results are expressed as mean ± S.E.M. *$p < 0.05$ vs. control group (CT); V – vehicle group (DMSO 0.5%).

2.8.2. Ligand design and optimization

The chemical structure of the 3-nitro and 4-nitro chalcones was drawn using the MarvinSketch code (Csizmadia, 2019), saved at physiological pH (Figure 1), and the lowest energy conformers were optimized using the Avogadro code (Hanwell et al., 2012), configured to use *steepest descent* algorithm with cycles of 50 iterations, applying the MMFF94 force field (*Merck Molecular Force Field*) (Batista de Andrade Neto et al., 2021; Halgren, 1996).

2.8.3. General docking procedures

To evaluate the mechanism of action of chalcone 1 (3-nitro) and 2 (4-nitro) against the GABAA receptor and of chalcone 2 (4-nitro) against the 5-HT3A channel, molecular docking simulations were performed, with the structures of receptors obtained from the Protein Data Bank repository (https://www.rcsb.org/), identified as "CryoEM structure of human full-length alpha1beta3gamma2L GABAAR in complex with diazepam (Valium), GABA and megabody Mb38" (PDB 6HUP) (Masiulis et al., 2019) and "Cryo-EM structure of 5HT$_{3A}$ receptor in presence of granisetron" (PDB 6NP0) (Basak et al., 2019). The preparation of protein structures was performed using the AutoDockTools code (Morris et al., 2009), where residues were removed and added to Gasteiger charges and polar hydrogen atoms (Silva Mendes et al., 2022; Yan et al., 2014).

Molecular docking simulations were performed using AutoDockVina code (Trott & Olson, 2010), configured to run the Lamarckian Genetic Algorithm (LGA) and *Exhaustiveness* 64 (Marinho et al., 2020). Fifty independent simulations were performed using a simulation grid centered on the target

in order to involve the entire protein structure with the axes: 125,281 (x), 139,534 (y) and 136,018 (z), size parameters 126 Å (x), 100 Å (y)) and 126 Å (z) with the GABAA receiver and axes: 159,615 (x), 159,705 (y) and 161,067 (z), size parameters 94 Å (x), 80 Å (y) and 126 Å (z) with channel 5- HT$_{3A}$. To validate the docking simulations, the redocking technique was performed with the drug Diazepam (DZP) (Silva Mendes et al., 2022) and granisetron (CWB) co-crystallized in the GABA$_A$ and 5-HT$_{3A}$ receptors, respectively.

The statistical parameter RMSD (*Root Mean Square Deviation*) with values up to 2.0 Å (Yusuf et al., 2008) and affinity energy, with values lower than −6.0 kcal/mol (Shityakov & Foerster, 2014; J. Silva et al., 2021), and the affinity energy was also used to assess the stability of the complexes formed. Using the values of the distances between the donor and acceptor atoms, it was evaluated the intensity of the Hydrogen bonds (H-Bond) classified as *Strong* bonds when they present distances between 2.5-3.1 Å, *Average* bonds between 3.1-3.55 Å and *Weak* bonds when they present length greater than 3.55 Å (Rose et al., 2018).

2.9. Molecular dynamic

Molecular dynamics (MD) simulations were performed with the NAMD program (Phillips et al., 2005). The best conformations obtained in molecular coupling were solved in water in the TIP3P model (Kato et al., 2021), in the CHARMM36 force field and addition of ions to neutralize the total system load. Finally, it was submitted to energy minimization by the Steepest Descent method. The system was then introduced to NVT and NPT balances under conditions described by Langevin (Farago, 2019). The system production simulations were performed with a time of 100 ns. The BLA was used as a reference ligand to analyze the interactions of the formed complex. The quality of the structures obtained in MDs was evaluated using the following parameters with NAMD:

- Potential Energy (kcal/mol) (Diez et al., 2014);
- Protein-Ligand Interaction Energy (kcal/mol);
- The mean quadratic deviation of the atomic positions of proteins, binders, and distances between them (RMSD, Å), and the mean quadratic deviation of the atomic positions of proteins, ligands, and distances between them (RMSD, Å);
- Hydrogen bonds were evaluated with Visual Molecular Dynamics (VMD) (Humphrey et al., 1996).
- The mean quadratic fluctuation of the minimum distances between proteins and ligands was observed in MD (RMSF, Å) (Arshia et al., 2021). The graphs were generated using the Qtrace program (Lima et al., 2012).

2.10. MM/GBSA calculations

On basis of MD log file of NAMD software (Phillips et al., 2005), the MM/GBSA was calculated by MolAlCal (Bai et al., 2021) and was estimated by the equations 1-3.

$$\Delta G_{bind} = \Delta H - T\Delta S \approx \Delta E_{MM} + \Delta G_{sol} - T\Delta S \qquad (1)$$

$$\Delta E_{MM} = \Delta E_{internal} + \Delta E e_{le} + \Delta E_{vdw} \qquad (2)$$

$$\Delta G_{sol} = \Delta G_{GB} + \Delta G_{SA} \qquad (3)$$

Where ΔE_{MM}, ΔG_{sol}, and $T\Delta S$ represent the gas phase MM energy, solvation free energy (sum of polar contribution ΔG_{GB} and nonpolar contribution ΔG_{SA}) and conformational entropy, respectively (Gohlke et al., 2003; Gohlke & Case, 2004). ΔE_{MM} contains Van Der Waals energy ΔE_{vdw}, electrostatic ΔE_{ele} and $\Delta E_{internal}$ of bond, angle, and dihedral energies. If there are no binding-induced structural changes in the process of MD simulations, the entropy calculation can be omitted (DasGupta et al., 2017).

2.11. Virtual screening of target classes

The two-dimensional structures of chalcones 1 and 2 were drawn in the Marvin JS drawing engine, built into the SwissTargetPrediction online server (http://www.swisstarget-prediction.ch/) to perform a virtual screening with known active structures (3 D/2D) against target classes and specific biological targets of the Rattus norvegicus organism, to conduct the structural analysis of molecular docking tests.

2.12. Phyisicochemical properties and medicinal chemistry

The two-dimensional drawings of the chalcones structures were submitted to the calculation of the acid ionization constant (pKa) of the academic license software MarvinSketch version 22.5, ChemAxon (https://chemaxon.com/products/marvin), to estimate the dominant microspecies in pH physiological (pH of approximately 7.4). Then, the substances were reported in linear notation of SMILES (Simplified Molecular Input Line Entry System) to the online server ADMETlab 2.0 (https://admetmesh.scbdd.com/), where the physicochemical properties of molecular weight were calculated. (MW), intrinsic lipophilicity (logP) and buffer (logD), solubility coefficient (logS), number of H-bond acceptors and donors (nHA and nHD), topological polar surface area (TPSA), number of rotating bonds (nRot), number of rings (nRing), number of atoms in the largest ring (MaxRing), number of hetaroatoms (nHet), formal charge (fChar), number of rigid bonds (nRig) and applied to the druglikeness criteria of the rules of (Lipinski, 2004), GSK (Gleeson, 2008), Golden Triangle (Johnson et al., 2009) and Pfizer's rule (Hughes et al., 2008).

2.13. In silico ADMET and toxicity prediction

2.13.1. Estimate of absorption and distribution
Through the regressions based on the structure of the online server ADMET Prediction Service (http://qsar.chem.msu.ru/admet/) the descriptors of human intestinal absorption (HIA%) and permeability coefficient in the blood-brain barrier (logBB) were associated with the structural contributions of the 4-Nitro and 3-Nitro chalcones, to estimate absorption and distribution. This prediction was supported by the estimation of passive permeability pharmacokinetic descriptors from the Madin-Darby canine renal cell model (P$_{app}$ MDCK),

P-glycoprotein substrate (P-gp), bioavailability fraction (F) and volume of distribution (VD) between blood plasma and biological tissues predicted in the ADMETlab 2.0 online server (https://admetmesh.scbdd.com/).

2.13.2. Site of metabolism and clearance

The two-dimensional structures of the chalcones were subjected to metabolism site prediction from the XenoSite online server substructure library (https://swami.wustl.edu/xenosite) to estimate the possible metabolites formed from phase I metabolism by cytochrome P450 (CYP450) isoforms, and phase II metabolism. The graphical response was supported by the prediction of CYP450 substrates and inhibitors (1A2, 2C19, 2C9, 2D6 and 3A4), intrinsic clearance rate of the non-liver microsome bound system ($CL_{int,u}$), and estimation of drug-induced liver damage (DILI) from the ADMETlab 2.0 server (https://admetmesh.scbdd.com/), to associate metabolism with the prediction of the lethal dose in rats (LD50) from the online tool ProTox-II (https://tox-new.charite.de/protox_II/).

2.13.3. Evaluation of hERG blockage and cardiotoxicity

Structural contributions likely to result in cardiotoxicity were assessed by the consensus test between the ADMET Prediction Service (http://qsar.chem.msu.ru/admet/) and Pred-hERG 4.2 (http://predherg.labmol.com.br/), where the affinity values (pKi) with hERG (human Ether-a-go-go-Related Gene) channels were associated with the 2D probability map for the fragments that present positive and negative structural contributions to blockade of hERG channels.

2.14. In vitro cytotoxicity on PC12 cells

For *in vitro* assays, the stock solutions of both molecules (0.05 M) were prepared with sterile DMSO, and working solutions were diluted with sterile PBS to guarantee a maximum of DMSO 0.5% in experimental groups. Cytotoxicity of present molecules in PC12 cells was assessed by MTT assay, as previously described (Mosmann, 1983). First, 20,000 cells/well were plated in 96-wells plates with 10% FBS DMEM (Dulbecco's Modified Eagle Medium) overnight, at 37 °C and 5% CO_2 atmosphere. After that, cells were treated with 3-NO_2 or 4-NO_2 (250 − 7.8 μM) for 24 hours. Then, experimental groups were incubated with MTT (2.5 mg/mL) for 4 hours and DMSO was added to solve the formazan salt. The absorbance was measured at 570 nm. DMSO 0.5% (vehicle group) and PBS were used as the negative control.

2.15. Statistical analysis

Results are expressed as mean values ± standard error of the mean for each group of six animals. After confirming normal distribution and homogeneity of the data, differences between the groups were subjected to analysis of variance (one-way ANOVA) and two-way ANOVA in experiments with antagonists, followed by Tukey's test. All analyses were performed using GraphPad Prism v.8.0 software. The level of statistical significance was set at 5% ($P < 0.05$).

3. Results

3.1. Toxicity

3.1.1. In vivo acute toxicity

Chalcones 1 and 2 were non-toxic to adult zebrafish up to 96 h of analysis ($LD_{50} > 10$ mg/kg). There was no death and did not cause any apparent anatomical changes in the animals.

3.1.2. In vitro cytotoxicity on PC12 cells

As shown in Figure 1, both molecules presented similar toxicity only in concentrations of 250, 125 and 62.5 μM.

3.2. Assessment of locomotor activity

The locomotion of the animals was altered by chalcones 1 and 2 [*$p < 0.05$, *** $p < 0.001$**** $p < 0.0001$, ##$p < 0.01$, ####$p < 0.0001$ *vs* naive or vehicle (1; 3 or 10 mg/kg)], as the animals had significantly reduced locomotor activity when compared to the control groups (naive and vehicle) (Figure 2A and B). The results did not differ significantly from the positive DZP control.

3.3. Anxiolytic evaluation

Chalcones 1 and 2 (1, 3 or 10 mg/kg) increased (**p < 0.01, ****$p < 0.0001$ or #$p < 0.05$, ##$p < 0.01$, ###$p < 0.001$, ####$p < 0.0001$ *vs* Naive or vehicle) the time of animals in the light region of the aquarium in the light/dark test (Figure 3A and B). A dose of 0.5 mg/kg of chalcone 2 was analyzed for anxiolytic effect and had no effect. Thus, we evaluated the
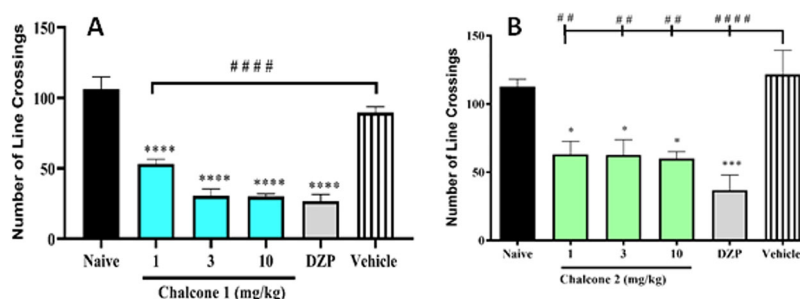
Figure 2. Effect of chalcone 1 (A) and chalcone 2 (B) on locomotor behavior of adult zebrafish in the Open Field Test (0–5 min). Values represent the mean ± standard error of the mean for 6 animals/group; ANOVA followed by *Tukey's* test (*$p < 0.05$, ***$p < 0.001$, ****$p < 0.0001$ vs Naive; ####$p < 0.0001$, ##$p < 0.01$; ####$p < 0.0001$, vs Vehicle).
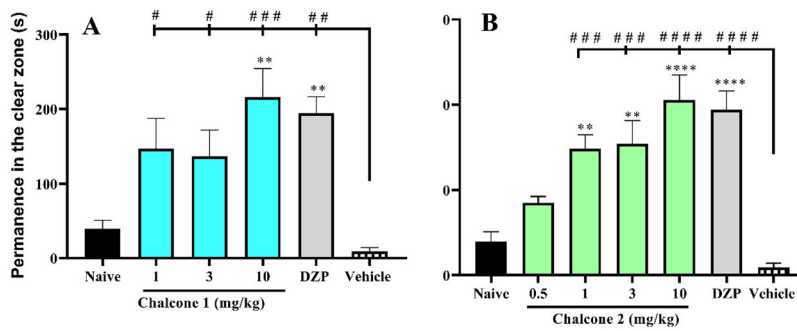
Figure 3. Effect of chalcone 1 (A) and chalcone 2 (B) on zebrafish anxiety in the light/dark test (0–5 min). Values represent the mean ± standard error of the mean for 6 animals/group; ANOVA followed by *Tukey's* test (**$p < 0.01$; ***$p < 0.001$; ****$p < 0.0001$ vs Naive; #$p < 0.05$; ##$p < 0.01$; ###$p < 0.001$; ####$p < 0.0001$ vs Vehicle).
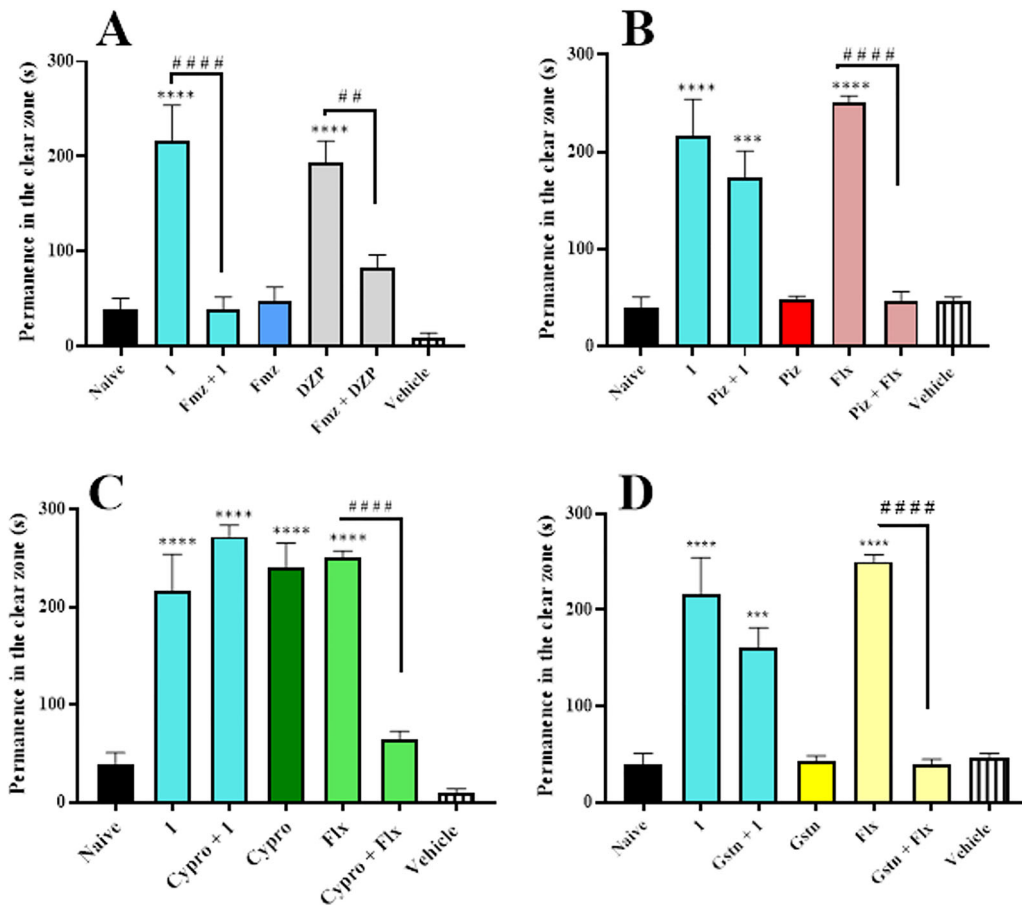
Figure 4. Effect of flumazenil (A), pizotifen (B), cyproheptadine (C) and granisetron (D) on the anxiolytic effect of chalcone 1 in the light/dark test. Values represent the mean ± standard error of the mean for 6 animals/group; ANOVA followed by Tukey's test (***$p < 0.001$; ****$p < 0.0001$ vs Naive or vehicle; ##$p < 0.01$, ####$p < 0.0001$ vs chalcone 1 or DZP or fluoxetine - Flx).

mechanism with the two lowest dosages of chalcone 2. It is important to emphasize that the dose of 10 mg/kg presented a superior result to the effect of Diazepam (DZP; 10 mg/kg), positive control.

3.4. Evaluation of GABAergic and serotonin neuromodulation

The mechanism of anxiety via GABAA was performed through pretreatment with flumazenil. The highest dose (10 mg/kg) of chalcones 1 and 2 and DZP (10 mg/kg) that caused anxiolytic behavior in the animals had this effect

reduced (#$p < 0.05$, ##$p < 0.01$, ####$p < 0.0001$ *vs* Chalcona **1** and **2** or DZP) by flumazenil, as the fish spent most of their time in the dark region of the aquarium demonstrating anxiety behavior (Figures 4A and 5A).

In addition, we evaluated the two lowest doses (1 and 3 mg/kg of chalcone 2) to verify the lowest dose capable of modulating GABAa activity and there was no modulation. The antagonists' pizotifen and cyproheptadine were not able to reverse the anxiolytic effect of chalcone **1** and **2**, unlike pretreatment with granisetron which caused (#$p < 0.05$ *vs* Chalcone **2**) anxiety behavior in animals treated with chalcone **2** (Figure 5D). Pretreatment with the 5-HT$_{1/2A/2C/3A/3B}$
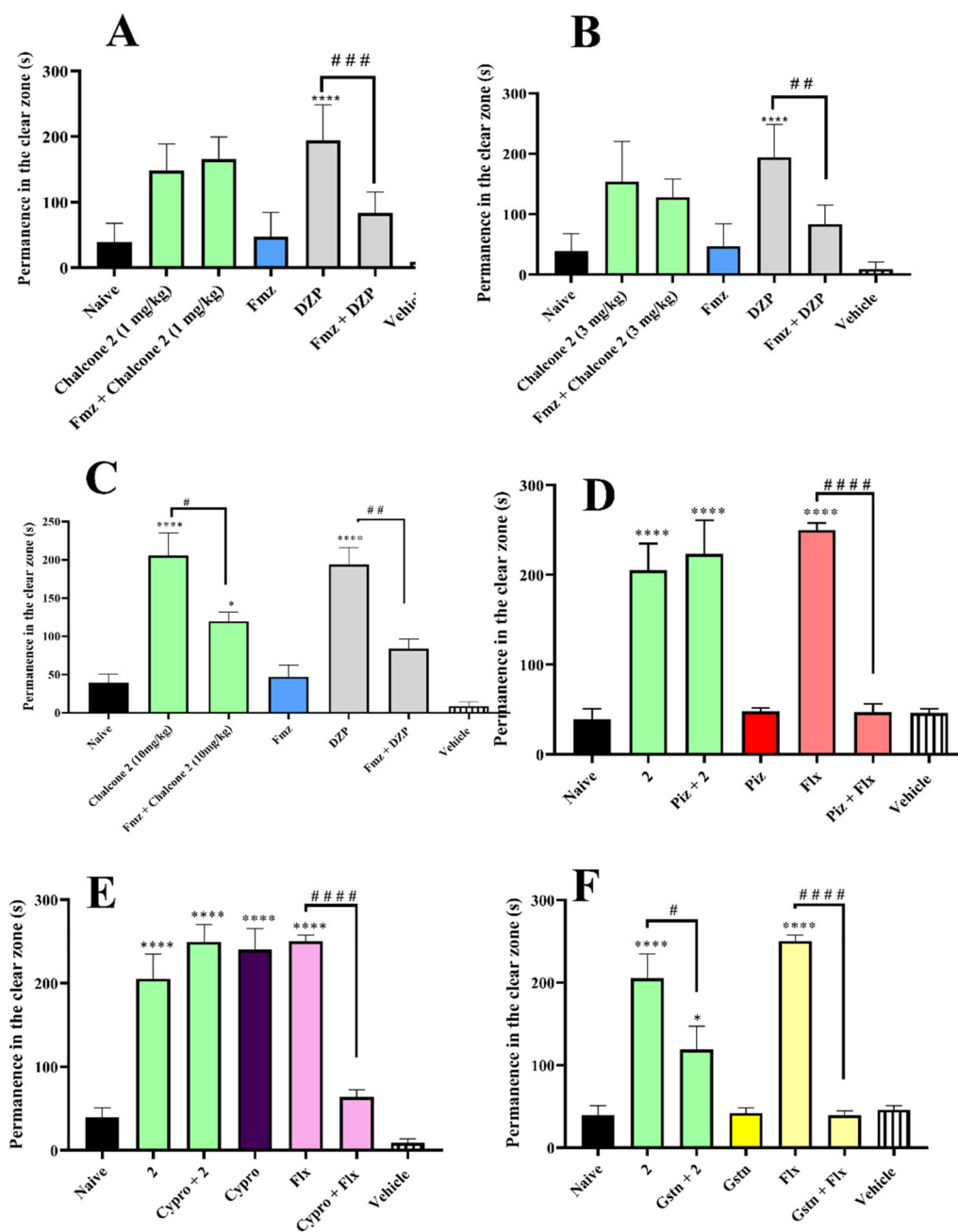
Figure 5. Effect of flumazenil (A), pizotifen (B), cyproheptadine (C) and granisetron (D) on the anxiolytic effect of chalcone 2 in the light/dark test. Values represent the mean ± standard error of the mean for 6 animals/group; ANOVA followed by Tukey's test (*$p < 0.05$, ****$p < 0.0001$ vs Naive or vehicle; #$p < 0.05$, ##$p < 0.01$, ####$p < 0.0001$ vs chalcone 2 or DZP or fluoxetine - Flx).

antagonists reversed (####$p < 0.0001$ vs Flx) the anxiolytic effect of fluoxetine (0.05 mg/kg) (Figures 4B–D and 5B–D).

3.5. Molecular docking

All simulations performed (docking and redocking) showed RMSD values lower than the reference value (2.0 Å), in the order of 1,721 Å (3-nitro/GABA$_A$), 1,699 Å (4-nitro/GABA$_A$), 1.02 Å (DZP/GABA$_A$), 1064 Å (4-nitro/5HT$_{3A}$) and 1664 Å (CWB-5HT$_{3A}$). Regarding the affinity energy, the chalcone 1/GABA$_A$, chalcone 2/GABA$_A$, DZP/GABA$_A$, 4-nitro/5HT$_{3A}$ and CWB-5HT$_{3A}$ complexes presented values in the order of −8.5 kcal/mol, −8.5 kcal/mol, −7.4 kcal/mol, −8.0 kcal/mol and −10.9 kcal/mol respectively.

Analyzing the interaction patterns against the GABA$_A$ receptor, it was possible to identify that the chalcone 1/GABA$_A$ complex is formed by five hydrophobic interactions, two with the nonpolar side chain of the Phe 77 C residue (3.74 and 3.99 Å) and three with the residues uncharged polar side chain Tyr 58 C (3.61 and 3.77 Å), Thr 142 C (3.91 Å) and an H-bond average with the uncharged polar side chain residue Ser 205 D (3.35 Å) (Figure 6). The chalcone 2/GABA$_A$ complex is formed by hydrophobic interaction with the uncharged polar side chain residue Tyr 58 C (3.61 Å), two *strong* H-bonds with the uncharged polar side chain residues Asn 60 C (2.32 Å), Ser 195 C (2.36 Å), a p-Stacking interaction with the nonpolar side chain of the aromatic residue Phe 77 C (3.77 Å) and a π-Cation interaction with the primary side-chain residue Lys 156 D (4.21 Å).
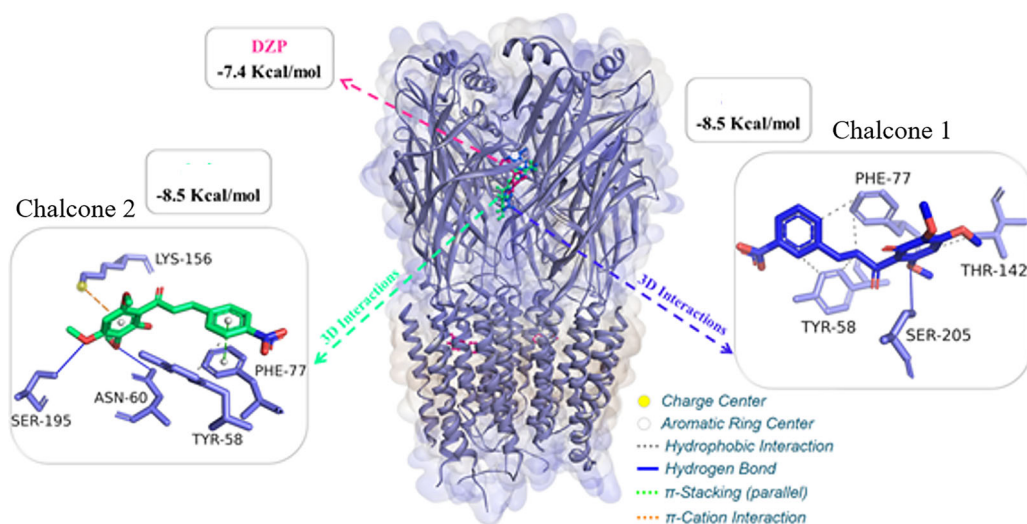
Figure 6. Complex of interaction between the GABA$_A$ receptor, chalcones 1 and 2 and the co-crystallized inhibitor diazepam (DZP).
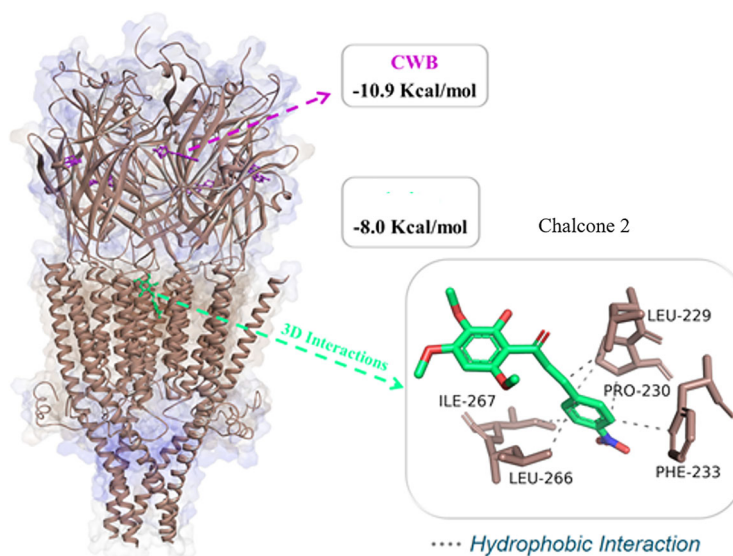
Figure 7. Complex of interaction between the 5-HT3A, 4-nitro receptor and the co-crystallized inhibitor granisetron (CWB).

Regarding the 5-HT$_{3A}$ channel, it was possible to identify that the chalcone 2/5HT$_{3A}$ complex is formed by six hydrophobic interactions with the nonpolar side chain of residues Leu 229 A (3.23 Å), Pro 230 A (3.69 and 3.72 Å), Phe 233 A (3.68 Å), Leu 266B (3.74 Å) and Ile 267B (3.65 Å). The granisetron binding site (CWB) co-crystallized between chains A and B in the 5-HT$_{3A}$ channel is formed by residues Asp 42 A, Val 43 A, Ile 44 A, Trp 63 A, Tyr 64 A, Arg 65 A, Asn 101B, Tyr 126 A, Thr 154B, Ser 155B, Trp 156B, Arg 169 A, Asp 177 A, Phe 199B, Ile 201B, Tyr 207B and Glu 209B. Chalone 2 complexes in a region different from the granisetron binding site (CWB), suggesting a possible synergistic effect (Figure 7).

3.6. Virtual screening of target classes

In this study, a structure-based virtual screening was applied to estimate the structural contributions of Chalcones 1 and 2 in their biological interactions. With the results, it was possible to observe that Chalcona 2 showed similarity with at least 15 3 D structures from the ChEMBL dataset with reported interaction with 5-HT system receptors, including the 5-HT$_{3A}$ ion transporter channel and the 5-HT$_{1A}$ receptor, and with 24 structures that show affinity with the GABA$_A$ target (Figure 8), with a substantial contribution from the *para*-nitrobenzene group (4-NO2). On the other hand, structures like the 3-Nitro analogue (chalcone 1) were not detected compared to the targets mentioned here.

3.7. Molecular dynamics

A thermodynamic system composed of solute and solvent can be represented by a protein-ligand-solvent-ion complex. In this system, there are interactions of various types (intermolecular forces), in addition to thermal exchanges between the molecules and the ions present; Thus, as dictated by the laws of thermodynamics, the relationship between these molecules and how heat transfer happens is related to several energy changes. From this, molecular dynamics
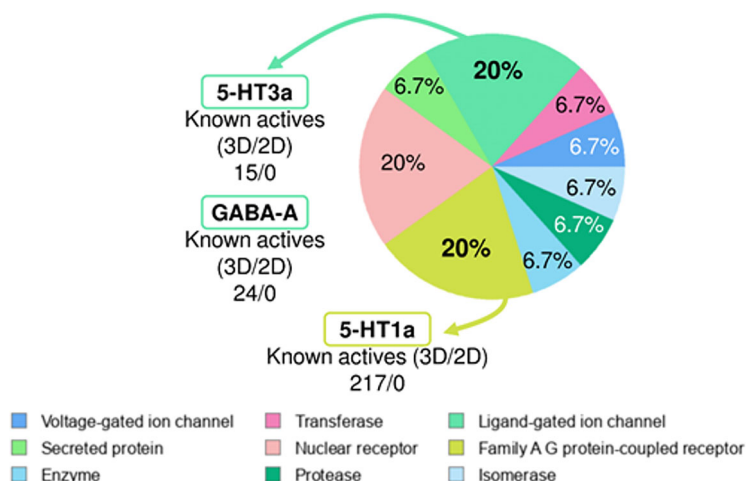
Figure 8. Structure-based virtual screening of target classes results.
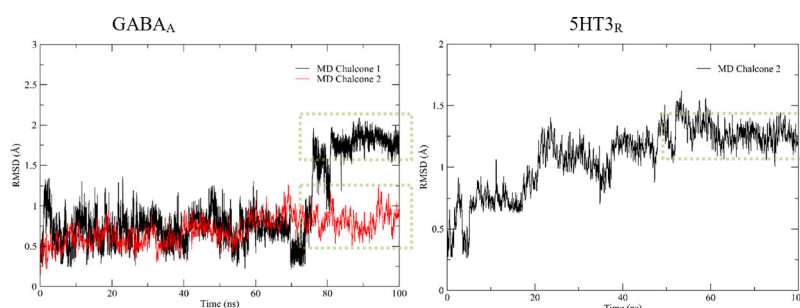
Figure 9. Root Mean Square Deviation (RMSD), concerning the initial confirmation of the ligand-enzyme complex versus the simulation time (ns) in the production simulations step of the MD with Chalcone 1/GABA$_A$ (black) and MD with Chalcone 2/GABA$_A$; MD with Chalcone 2/5HT3$_R$ (black).

simulations were performed with protein-ligand complexes through NAMD to evaluate possible global conformational changes and protein stability after each conformation and to obtain information on the mechanism of interaction of the complexes at the molecular level.

3.7.1. RMSD analysis
Soon after molecular docking was performed, chalconas 1 and 2 were selected because they had the best binding energies to perform the molecular dynamics study, according to the catalytic site of GABA$_A$ and 5HT3$_R$ (Figure 9). It was observed that the mean RMSD values for all 100 ns simulations in the production stages were around 0.63 Å for Chalcone 2/GABA$_A$. For Chalcone 1, with the same protein was only achieved from 74 ns, with average RMSD of 1.72 Å. However, in the MD of the Chalcone 2/5HT3R complex, stability was practically only achieved from the time of 41 ns, along its trajectory, not exceeding the mean value of 1.25 Å; this is justified in previous studies, which performed MD simulations to verify the stability of the HIV-1 protease enzyme in an aqueous solution with different ligands containing different levels of α helix and β leaves. Therefore, these long-range interactions were calculated using the SPME procedure and a Langevin thermal bath at 310 K. The conformational alterations of the protein observed during MD simulations were described by means of mean quadratic deviations (RMSD) in equation 5. $r_i(t)$ and $r_i(0)$ are the coordinates of

the i-th atom at time t and 0, respectively, and N is the number of atoms in the domain of interest.

$$RMSD = \left[\frac{1}{N} \sum_{i=1}^{N} \left[r_i(t) - r_i(0)^2 \right] \right]^{1/2} \tag{5}$$

3.7.2. RMSF analysis
From the RMSD analysis it was possible to verify the stability of the complexes. However, it was necessary to obtain the conformational alterations of the protein observed during the MD simulations, based on fluctuations in the mean structure of the protein, expressed in terms of fluctuations of the mean atomic quadratic deviations (RMFS), which were calculated according to equation 6. Where $\overline{r_i}$ are the coordinates of the ith atom in the time step j, $\overline{r_i}$, their average positions, and I is the time of simulations, expressed as the total number of time steps collected.

$$RMSF_i = \left[\frac{1}{\mathfrak{I}} \sum_{j=0}^{\mathfrak{I}} \left[\overline{r_i}(j) - \overline{r_i} \right]^2 \right]^{1/2} \qquad Eq. 6.$$

The RMSF of the system was performed to understand the displacement and stability of each protein residue in the trajectory of the 100 ns simulation. Figure 10 overlaps with the main interactions of the leading complexes studied (Chalcone 1 and 2). Thus, it can be concluded that there were significant conformational alterations of the ligant-GABA$_A$ and ligant-5HT3$_R$ complexes during the simulation
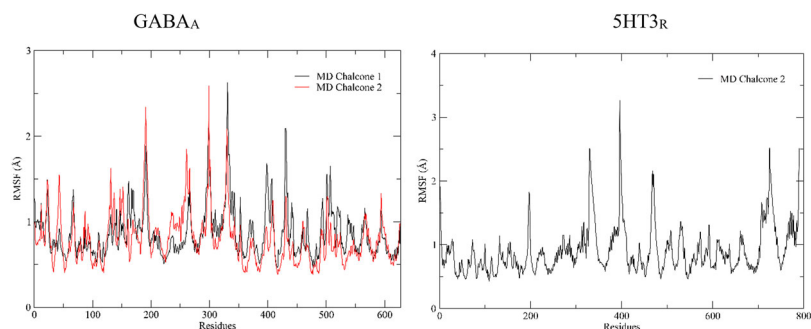
Figure 10. Root Mean Square Fluctuation (RMSF), concerning the initial confirmation of the ligand-enzyme complex versus the simulation time (ns) in the production simulations step of the MD with Chalcone 1/GABA$_A$ (black) and MD with Chalcone 2/GABA$_A$; MD with Chalcone 2/5HT3$_R$ (black).
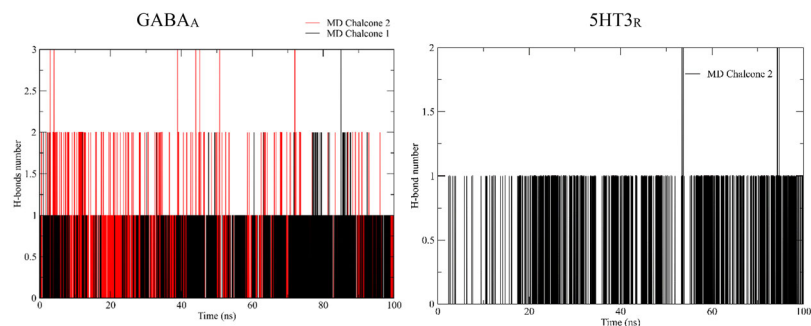
Figure 11. Hydrogen bonds formed between the protein and the ligand during the simulation steps.

times. For the GABA$_A$ complex, the results suggest that the trajectories of molecular dynamics simulations for all complexes after the production stages presented mean oscillations with significant correlations with critical residues in replication. The two complexes formed between ligands and GABA$_A$ presented values higher than 2.0 Å from the residue from Tyr 199 to Thr 440. The complexes formed between the ligant and 5HT3$_R$ gave values higher than 2.0 Å in the residues Trp 320, Arg 400, Ile 440, and Leu 720. Despite the fluctuations presented, the results showed good stability of the structures in an aqueous solution. The conformations obtained in the MD simulations for both proteins were complexed with various ligands through docking techniques, generating important information about the binding modes of small molecules in the different states of enzyme folding.

3.7.3. H-bonds analysis
The number of hydrogen bonds is essential to verify whether a complex has reached stability in a dynamic system. After the 100 ns, it was possible to verify the hydrogen bonds formed between GABAA proteins and 5HT3R with their respective simulated ligands in long stages of production in molecular dynamics, in Figure 11. During the simulation, there were changes in hydrogen binding networks, and the number of interactions fluctuated between 2 or 3 for GABAA and 1 or 2 for 5HT3$_R$. In the GABA$_A$ complex with Chalcone 1, the isolated hydrogen bonds and the moderate average number of hydrogen bonds per period (up to 2 bonds) suggested that hydrogen bonding networks were relatively adequate and median. It was forming reasonable connections during its trajectory. Chalcone 2 MD was shown to have more interactions along the course (3 links), suggesting

another hydrogen binding network, moderately more significant than the previous one.

For the simulation of Chalcone 2 with the 5HT3$_R$ protein, a maximum of 2 hydrogen bonds were formed, characterizing a relatively weaker network of interactions. The moment when these connections were very present suggests that this interaction maintained the stability of the complex beyond the size of the compounds and their functionalities.

Therefore, complementary correlations can be observed in comparing hydrogen bonds formed in molecular dynamics with those previously obtained by the coupling process, indicating the convergence of a static method for a continuous system process.

3.7.5. MM/GBSA calculations
Calculating the free energies of a receptor complex can be done by calculating molecular mechanics energies combined with the generalized Born and surface area continuum solvation (MM/GBSA). MolAICal, therefore, is a computational tool that quickly estimates the free energy of a system, without ligand entropy, based on the approach of three trajectories obtained by molecular dynamics. The Chalcone 1/GABA$_A$ complex was the best result, based on its free energy, with −29.41 kcal/mol, about the other linker under study, Chalcone 2/GABA$_A$, which presented a free energy of −21.82 kcal/mol. In the other current simulation, the Chalcone 2/5HT3$_R$ complex gave free energy, with −30.68 kcal/mol (as showed in the Table 1). The term entropy variation concerns the loss of degrees of freedom resulting from the formation of one or more interactions because previously, there were only two molecules (ligand and protein), which could access any degrees of rotational,

translational, or vibrational freedom, now there is a complex where the movement of molecules is much more limited.

This estimate can then be obtained from the calculations of normal modes for the two systems. Thus, for a macromolecular complex with a target and a ligand, the interaction energy must be estimated according to equations 7, 8, and 9.

$$\Delta A_{interaction}^{(vac)} = \left(E_{complex}^{MM} - E_{target}^{MM} \right) - \left(E_{complex}^{MM} - E_{ligand}^{MM} \right)$$
$$+ T\Delta S_{NORMODS} \tag{7}$$

$$\Delta A_{interaction}^{(vac)} = E_{complex}^{MM} - E_{target}^{MM} - E_{complex}^{MM} + E_{ligand}^{MM} + T\Delta S_{NORMODS} \tag{8}$$

$$\Delta A_{interaction}^{(vac)} = E_{ligand}^{MM} - E_{target}^{MM} + T\Delta S_{NORMODS} \tag{9}$$

3.8. Physicochemical properties and medicinal chemistry

3.8.1. pKa estimation and major microspecies
In Figure 12, it is possible to observe the distribution of the Chalcones microspecies and the influence of the difference

Table 1. Free energy estimation data of chalcones against GABA$_A$ and 5HT3$_R$.

Complex	$\Delta E_{ele} + \Delta G_{sol}$ (kcal/mol)	ΔE_{vdw} (kcal/mol)	ΔG_{bind} (kcal/mol)	Standard deviation
Chalcone 1/GABAA	14.33	−43.74	−29.41	+/− 0.0249
Chalcone 2/GABAA	13.60	−35.42	−21.82	+/− 0.0211
Chalcone 2/5HT3R	11.34	−42.01	−30.68	+/− 0.0208

in position of the substituent nitro group (4-NO$_2$ and 3-NO$_2$), in the aromatic ring B of the structures, in their ionization states. With the analysis, it is possible to observe that Chalcone 1 had the lowest pKa value (7.26) concerning Chalcone 2 (7.76) (Figure 12A), indicating that its chemical equilibrium shifts toward the predominance of the anionic species at pH physiological (pH of approximately 7.4), in a relative concentration in the order of 58.14% with the conjugate base of Chalcone 2 (30.51%) (Figure 12B), behavior associated with the meta-directing effect of the 3-NO$_2$ substituent that facilitates the deprotonation of the 2-OH group of ring A, when compared to the 4-NO$_2$ substituent.

3.8.2. Estimate of drug-likeness
The filter that combines physicochemical properties commonly used to estimate the drug-likeness of new drug candidates can be visualized in Figure 12 and Table 2. In a visual inspection of the radar in Figure 12C, it is possible to note that both Chalcone 1 (4-Nitro) and the analogue Chalcone 2 (3-Nitro) are within the molecular weight and lipophilicity spectrum of Lipinski's "rule of five" and GSK's rule (MW $\leq$ 400 $\sim$ 500 g/mol and logP $\leq$ 4 $\sim$ 5), suggesting a favorable profile of ADMET. In Figure 12D, it is possible to observe that the alignment between these properties guarantees an optimization in the attributes of passive permeability and

Figure 12. Estimate of pKa values of 1 and 2 Chalcones (A), microspecies distribution as a function of the pKa estimation (B), drug-space of the drug-likeness estimation (C) and estimate of oral absorption and clearance by the Pfizer's drug-space (D).

Table 2. Prediction of the physicochemical properties and estimate of drug-likeness of the Chalcones 1 and 2.

Property	Chalcone 1	Chalcone 1
Molecular weight	359.1 g/mol	359.1 g/mol
logP	2.96	2.99
logS	−5.05 mol/L	−5.14 mol/L
logD	2.71	2.75
nHA	8	8
nHD	1	1
TPSA	108.13 Å^2	108.13 Å^2
nRot	7	7
nRing	2	2
MaxRing	6	6
nHet	8	8
fChar	0	0
nRig	15	15
Lipinski rule	Accepted	Accepted
Pfizer rule	Accepted	Accepted
GSK rule	Accepted	Accepted
Golden Triangle	Accepted	Accepted

Note: nHA (number of H-bond Acceptors); nHD (number of H-bond Donors); TPSA (Topological Polar Surface Area); nRot (number of Rotatable Bonds); nRing (number of Rings); MaxRing (number of atoms in the biggest ring); nHet (number of Heteroatoms); fChar (formal charge); nRig (number of Rigid bonds).

Table 3. Predicted ADME properties in the ADMETlab 2.0 web server and oral acute toxicity in the ProTox-II web tool to the 4-Nitro and 3-Nitro chalcone analogues.

ADME property	Chalcone 1	Chacone 2
P_{app} MDCK	1.5×10^{-5} cm/s	1.4×10^{-5} cm/s
P-gp substrate	—	—
$F_{30\%}$	High	High
VD	0.39 L/kg	0.39 L/kg
Metabolism	CYP1A2 (+++)	CYP1A2 (+++)
	CYP2C9 (+++)	CYP2C9 (+++)
CYP1A2 inhibitor	++	++
CYP2C19 inhibitor	++	+
CYP2C9 inhibitor	++	++
CYP2D6 inhibitor	–	–
CYP3A4 inhibitor	++	++
$CL_{int,u}$	7.789 mL/min/kg	7.369 mL/min/kg
DILI	++	++
LD50	3000 mg/kg	3000 mg/kg
Toxicity class	5	5

Note: P_{app} MDCK (Passive permeability predicted by the Madin-Darby Canine Kidney cells model); P-gp (P-glycoprotein); $F_{30\%}$ (Fraction of bioavailability > 30%); VD (Volume of distribution); CYP (Cytochrome P450 isoforms); $CL_{int,u}$ (Clearance); H-HT (Human hepatotoxicity). +++ (poor result) and –– (good result).

metabolic stability of the Chalcones ($200 < MW \leq 500$ g/mol and $-2 < logD \leq 5$) since the ionization of the compounds was beneficial for the decrease in relative lipophilicity, observed by the relationship between logD at pH $7.4 < logP$ (Table 2). In addition, the H-bond acceptor groups (8 HA heteroatoms in total), including the methoxy and nitro substituents, strongly contribute to the topological polarity of the Chalcones in the order of 108.13 Å^2, occupying a physical-chemical space with low toxic incidence, within Pfizer's physical-chemical space (TPSA > 75 Å^2).

When analyzing the aromaticity of Chalcones, it was possible to observe that the total of 2 aromatic rings (nRing) is sufficient for an alignment between attributes that allow their development as a drug within the range of relative lipophilicity obtained for the substances, leading to a balance between lipid solubility, flexibility (7 nRot) and pharmacokinetic parameters.

3.9. In silico ADME and toxicity prediction

3.9.1. Estimate of absorption and distribution
The ADME prediction results can be visualized through the pharmacokinetic descriptors in Table 3 and graphically in Figure 13. With the analysis, it is worth noting that Papp values $> 10 \times 10^{-6}$ cm/s suggest a high passive permeability of chalcones, which are organized in the order of chalcone 1 > Chalcone 2, ensuring greater human intestinal absorption (HIA) for the chalcone 1 (85.04%), concerning chalcone 2 (81.16%) (Figure 13A), in agreement with the estimated oral bioavailability fraction (F) of at least 30% (Table 3) and with the graphical estimate in Figure 12B.

In addition, the sizeable polar surface of chalcones can make it difficult for substances to access biological tissues, including the blood-brain barrier (BBB). The results show that permeability values at BBB (logBB) > -1.0 guarantee the access of at least 10% of the molecular fraction of the compounds in the central nervous system (CNS) (Fig. Yb),

corroborating the low volume of the estimated distribution of 0.39 L/kg for both derivatives (Table 3).

3.9.2. Site of metabolism and clearance
In the 2 D probability map in Figure 13C, it is possible to observe the main structural contributions of the chalcone analogs 1 and 2 in their metabolism and excretion processes. With the results, it is possible to observe that both molecules tend to form secondary metabolites from O-dealkylation reactions of the 3-OCH3, 4-OCH3 and 6-OCH3 groups, mainly by the CYP1A2 and CYP2C9 isoforms of the hepatic microsomes (HLM), constituting more water-soluble chemical entities for excretion. It is worth noting that the conjugate base (O–) of chalcone 1 is a species that is more readily excreted, and for this reason, a phase II biotransformation is unlikely. In contrast, the majority neutral species (OH) of chalcone 2 tends to form a conjugate much more water-soluble by UGT-mediated glucuronidation in phase II metabolism. This characteristic is easily noticed by the intrinsic clearance values ($CL_{int,u}$) estimated, where the majority species of chalcone 1 (7,789 mL/min/kg) tend to be released faster than its analogue chalcone 2 (7,369 mL/min/kg). In addition, the substances have, at the same time, a tendency to inhibit their metabolism pathway and the CYP3A4 isoform and may change the plasma concentration in case of co-administration of both or other CYP450 substrates, leading to a pharmacokinetic model based on in the control of the administered oral dose, estimated at 3000 mg/kg for the two substances, belonging to class 5 toxicity ($LD_{50} > 2000$ mg/kg), where toxicity by ingestion is unlikely (Diaza et al., 2015) (Table 3).

3.9.3. Evaluation of hERG blockage and cardiotoxicity
From the results of the prediction of the cardiotoxicity model, it is possible to observe that the chalcones presented affinity values (pKi) in the order of 5.5, classified as moderate by the statistical regressions based on structure, as shown in
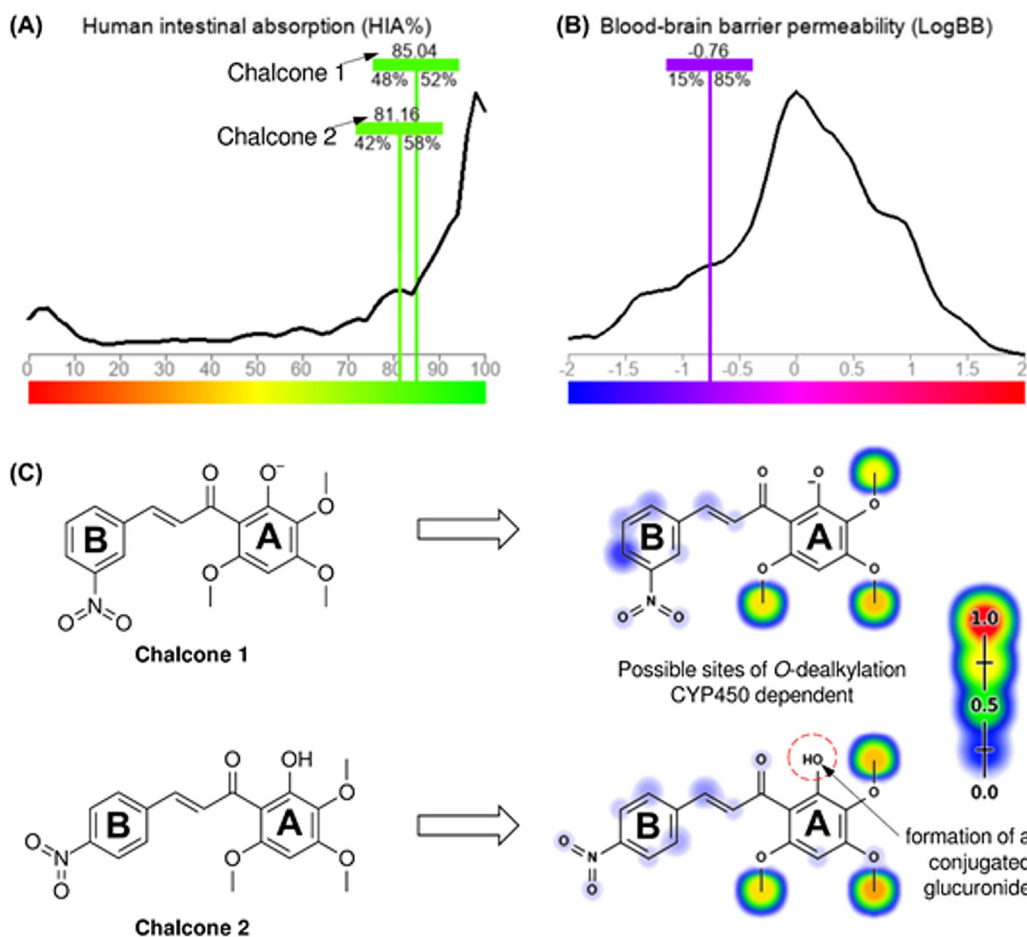
Figure 13. Estimation of human intestinal absorption (HIA%) (A), permeability coefficient at BBB (logBB) (B) and structural contributions of metabolic processes of the majority species of chalcones 1 and 2 (C).
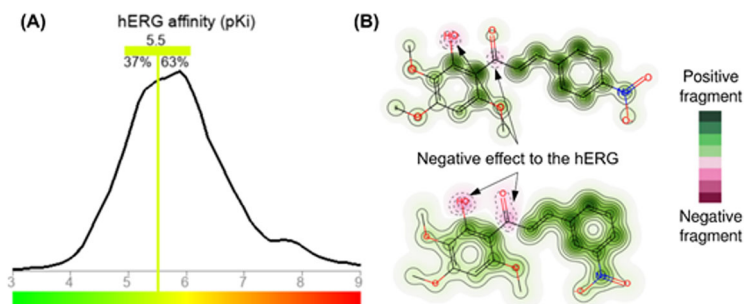
Figure 14. Statistical regressions (A) and structural analysis (B) for estimation of cardiotoxic potential of chalcones 1 and 2.

the graph in Figure 14A. Such behavior is observed in the 2 D probability map in Figure 14B, where the carbonyl and 2-hydroxy groups constitute negative structural contributions (magenta color) capable of blocking hERG channels. However, the hydrophobic contributions of the unsaturation of the aliphatic chain and the aromatic rings (green color) in the two molecules make the cardiotoxic response unlikely, decreasing their hERG blocking potentials.

4. Discussion

Chalcones did not show toxicity up to 96 h and agreed with studies carried out by (Maria Kueirislene Amâncio Ferreira et al., 2021), where they analyzed the acute toxicity by the same model, and studies designed by (Rani et al., 2021), which evaluated the toxicity of several chalcones in mice. Previous studies showed that chalcone (E)-3-(furan-2-yl)-1-(2hydroxy-3,4,6-trimethoxyphenyl)prop-2-en-1-one was evaluated for cytotoxicity *in vitro* in PC12 cells by the MTT assay under different concentrations and high cell viability was demonstrated indicating absence of cytotoxicity (Silva Mendes et al., 2022). In agreement with these findings, the two chalcones analyzed in this work were also acutely nontoxic up to 96 h of analysis.

In neuroscience research, studies of neuroprotection, neurotoxicity, neuroinflammation, neurosecretion and

synaptogenesis, PC12 cell line is one of the most used due to their corroboration with *in vivo* findings (Wiatrak et al., 2020). In present research, the both nitrochalcones presented similar toxicity on neuronal cells. Previously, toxicity of furanyl and dimethoxychalcone were assessed in PC12 cells, showing low decreasing of cell viability, with interesting neuroprotective effects (Silva Mendes et al., 2022).

The zebrafish experimental model has contributed to studying several pathologies that affect the human brain, including neurodevelopmental, psychotic and neurodegenerative disorders (Cosacak et al., 2017). It has contributed to a better understanding of the standard and evolutionarily conserved mechanisms of Central Nervous System (CNS) disorders and contributes to behavioral research and screening for new drugs that act in the CNS (A. M. Stewart et al., 2014). These studies are essential because they establish functional links between neurochemistry and behavior in vertebrate species (Bugel & Tanguay, 2018).

In this sense, the effect of chalcones **1** and **2** on zebrafish behavior was evaluated through the open field test, and all doses promoted changes in animal locomotion. This parameter of behavior evaluation is characteristic of drugs that act on the zebrafish CNS (Gupta et al., 2014). However, the change in locomotion can also be a sedation response caused by the influence of the drug administration route, usually influenced by the time of action, intensity and duration (Cachat et al., 2011; A. Stewart et al., 2012).

Thus, given this question, the anxiolytic effect of chalcones **1** and **2** was investigated by the light and dark test, as it is specific for the evaluation of anxiety in a zebrafish model (Maximino et al., 2010). Animals naturally have an aversion to the light zone of the aquarium, staying in the dark zone, as the dark zones offer camouflage against potential natural predators when in their natural habitat (Maximino et al., 2010; A. Stewart et al., 2011). Thus, when the animals were treated by *v.o* with chalcones **1** and **2** at all doses, there was an increase in the time spent in the clear zone of the aquarium, as observed with the group that received DZP at a dose of 10 mg/kg. Chalcones **1** and **2** at doses of 10 mg/kg showed anxiolytic effects superior to DZP. According to Higgs et al. (2019) According to Higgs et al. (2019), most anxiolytic compounds carry as substituent groups: hydroxyl (-OH), methoxy (-OCH$_3$), methyl (-CH$_3$), dimethylamine (-N(CH$_3$)$_2$, halogens (F, Cl, Br, I) and nitro (-NO$_2$) In the chalcones of this study, the presence of groups (-OH, OCH$_3$, NO$_2$) in rings A and B can be evidenced.

According to what is reported in the literature, the anxiolytic action of chalcones can occur through neurotransmission via GABA$_A$Rs (Maria Kueirislene A. Ferreira et al., 2019; Maria Kueirislene Amâncio Ferreira et al., 2021). Most GABA$_A$Rs are composed of two α, two β and one γ2 subunit (Golani et al., 2022). Flumazenil is a competitive antagonist of BZDs because it binds in the same region in GABAAR and is used in the clinic for the treatment of overdoses of benzodiazepines (Hood et al., 2009), it has been used in several studies to evaluate the mechanism of action of flavonoids with anxiolytic effect via GABA$_A$R (A. W. da Silva, Ferreira, Pereira, et al., 2021; Maria Kueirislene Amâncio Ferreira et al.,

2021). In silico studies show that flumazenil binds at the $\alpha + \gamma$- interface of GABAAR in an entirely different conformation from Diazepam and Alprazolam, interacting with a part of the overlap region of BZDs (Golani et al., 2022), this binding is sufficient to block the effects of benzodiazepines on the GABA$_A$ receptor, which makes it essential to study drugs with anxiolytic effects through this pathway. The animals treated with the highest dose of chalcones **1** and **2** (10 mg/kg) had their anxiolytic behavior blocked by pre-treatment with flumazenil, similar to the DZP group pre-treated with flumazenil, as they returned to remain most of the time in the area preta aquarium, anxiogenic behavior, these findings may indicate that the anxiolytic effect of chalcones **1** and **2** are mediated by the GABAergic transmission system, similar to the result of Cho et al. (2011) who showed the anxiolytic action of the natural chalcone isoliquiritigenin (2′,4′,4-trihydroxychalcone) which also acts on the BZD binding site of the GABA$_A$ receptor.

The chalcones in this work are derived from the natural compound 2-hydroxy-3,4,6-trimethoxyacetophenone, which has an anxiolytic activity mediated by serotonin receptors (A. W. da Silva et al., 2021). Chalcones **1** and **2** present structural differences; they are epimers, that is, the difference between them is in the position of the nitro group (NO$_2$) that are in the **m** and **p** positions in the B ring of the chalcones, respectively (Figure 1). The presence of ring **B** in chalcone **2** with the substitution of an atom of (H) by the group (-NO$_2$) in the **para** position seems to potentiate the anxiolytic effect in the three doses when compared to chalcone **1** (Figure 3), allowing this effect through in GABAergic and serotonergic neuromodulation (Figure 5A and D).

Virtual screening based on a chemical structure is a predictive technique aided by machine learning functions that can conduct molecular docking tests. These functions are capable of performing similarity tests with ligands deposited in databases, with activity characterized against target classes or specific targets, to estimate the biological activity of a new drug candidate.

Therefore, by molecular docking, it was observed that the binding site of Diazepam co-crystallized between the C and D chains of the GABA$_A$ receptor is formed by residues Tyr 58 C, Asn 60 C, Phe 77 C, Phe 100 D, His 102 D, Ser 159 D, Tyr 160 D, Glu 189 C, Val 203 D, Gln 204 D, Ser 205 D, Ser 206 D and Tyr 210 D (Masiulis et al., 2019; Rose et al., 2018). The evaluated chalcones complex in the same region of the binding site of Diazepam, having common interactions with residues Tyr 58 C, Phe 77 C and Ser 205 D (Chalcone **1**, 3-nitro); Tyr 58 C, Asn 60 C and Phe 77 C (Chalcone **2**, 4-nitro), indicating similar action in the same DZP binding region at the GABA$_A$ receptor (Figure 6). A significant binding of chalcone **1** to residue Ser 205 D of the α1 chain of the GABAA receptor was observed, this is a fundamental region of the binding pocket of BZDs (Oliveira et al., 2018), which supposedly explains the anxiolytic effect of this chalcone. Types of flavonoids (flavones) were considered potential ligands for the binding site of benzodiazepines, as they exhibited coincident poses with more than 60% frequency in GABA$_A$, with the best pose having the B ring pointing to the hydrophobic

region of $_{\alpha1}$ Tyr159, $_{\alpha1}$ Phe99 and $_{\gamma2}$ Phe77 and $_{\alpha1}$ His101 (Oliveira et al., 2018), the chalcones studied here also had their B rings linked to the Phe77 residue of the $\gamma2$ chain of the active site, corroborating the anxiolytic effects identified in adult zebrafish.

Serotonin is one of the most critical neurotransmitters in the CNS that involves various cognitive and non-cognitive behaviors such as mood, sex, appetite, sleep, memory, emotion and anxiety (Chegini et al., 2014). 5-HT is produced and released by neurons that have their cell bodies in the raphe nuclei in the brain stem (Chegini et al., 2014). The 5-HT$_3$ receptor has two subunits known as 3 A and 3B, and it is the only ligand-gated ion channel serotonergic receptor that, when activated, causes an influx of Na$^+$and Ca^{2+}ions (Costall & Naylor, 2004). 5-HT$_3$ receptor antagonists demonstrate consistent effects ranging from anxiolytic to anxiogenic (Olivier et al., 2000), and being able to block postsynaptic receptors, facilitating and enhancing neurotransmission of serotonin that binds to other 5-HT receptors, especially 5-HT$_{1B}$ and 5-HT$_{2C}$ (Rajkumar & Mahesh, 2010). Granisetron is a 5-HT$_{3A/3B}$ receptor antagonist that causes anxiety in adult zebrafish (Maria Kueirislene Amâncio Ferreira et al., 2020; Gonçalves et al., 2020). In this study, pretreatment with granisetron blocked the anxiolytic effect of chalcone **2** but did not block the effect of chalcone **1**. Supposedly, the B ring of chalcone **2** with the substituent (-NO$_2$) in the **para** position, in addition to acting on GABA$_A$R, binds to the 5-HT$_{3A/3B}$ receptor activating the channel allowing the influx of ions and/or increasing serotonin neurotransmission that binds to other 5-HT receptors causing the anxiolytic effect. However, pretreatment with other 5-HT pathway antagonists (pizotifen and cyproheptadine) did not block the anxiolytic effect of the chalcones (Figures 4B and C; 5B and C).

The granisetron binding site (CWB) co-crystallized between chains A and B in the 5-HT$_{3A}$ channel is formed by residues Asp 42 A, Val 43 A, Ile 44 A, Trp 63 A, Tyr 64 A, Arg 65 A, Asn 101B, Tyr 126 A, Thr 154B, Ser 155B, Trp 156B, Arg 169 A, Asp 177 A, Phe 199B, Ile 201B, Tyr 207B and Glu 209B (Basak et al., 2019; Rose et al., 2018). Chalcone 2 (4-nitro) complexes in a region different from the granisetron binding site (CWB), suggesting a possible synergistic effect (Figure 7), demonstrated by six hydrophobic interactions with the non-polar side chain of residues Leu 229 A (3.23 Å), Pro 230 A (3.69 and 3.72 Å), Phe 233 A (3.68 Å), Leu 266B (3.74 Å) and Ile 267B (3.65 Å) of the 5-HT$_{3A}$ channel with the B-ring of the chalcone.

The importance of electron-withdrawing groups (-NO$_2$) in the B ring of the chalcones in the **m** and **p** positions is highlighted since it was observed that the position of the substituent was necessary for the modulation of anxiolytic activity. This explains the great affinity of 4-Nitro chalcone associated with similarity with at least 15 ligands of 5-HT$_{3A}$ channels, with a substantial contribution from the carbonyl group, and with 8 ligands of GABA$_A$ receptors that contain nitrobenzene in their molecular structure, constituting a predictive model capable of driving the structural contributions of 4-Nitro and 3-Nitro analogs with these receptors.

As a general rule of thumb for drugs, uncharged compounds that are small and low lipophilic are better absorbed in physiological compartments, whereas, in anonic compounds, this absorption is limited as the polar surface (TPSA) approaches 150 Å^2. Thus, Lipinski's commonly used "rule of five" suggests that compounds with logP $\leq$ 5, MW $\leq$ 500 g/mol, less than 5 H-bond donors (NH + OH) and less than 10 H-bond acceptors (N + O) present a balance between lipid solubility and permeability, ensuring an optimal drug-likeness profile. These physicochemical thresholds relate molecular weight and lipophilicity to the ionization state of a compound to achieve a physicochemical space of enhanced ADMET properties, such as bioavailability, distribution, metabolism and toxicity. In this study, it was possible to correlate the structural properties of chalcones 1 and 2 to justify the viability of the substances to act as drugs, especially orally. Furthermore, the satisfaction of the conditions imposed by the drug-likeness criteria, which combines the filters commonly used in medicinal chemistry, favors the alignment between the ADMET properties of the chalcones.

Exploited over the years by pharmaceuticals Pfizer, Inc., the molecular weight and logD properties estimated at physiological pH (pH of approximately 7.4) easily replace other physicochemical properties, such as TPSA and H-bond donor/acceptor, to relate the molecular size and relative lipophilicity of the majority microspecies of a substance, since the alignment between them guarantees the satisfaction of fundamental attributes of ADMET and access to the CNS with low toxic incidence: high passive permeability (P$_{app}$ > 10×10^{-6} cm/s) and low metabolic clearance (CL$_{int,u}$ < 100 mL/min/kg), associated with compounds with excellent oral absorption and metabolic stability. With the results explored here, it was possible to observe that the physicochemical properties of the two chalcones are in line with their pharmacokinetic parameters, guaranteeing pharmacological feasibility for the mechanism of action in the CNS.

Predicting drug candidate metabolism sites allows us to assess the harmful effect of metabolites formed by the oxidative mechanisms of phase I metabolism, mediated by cytochrome P450 (CYP450) isoforms and water-soluble conjugates of phase II metabolism. CYP450 substrates can lead to liver damage (DILI), while CYP450 inhibitors depend on controlling the daily dose administered in the hepatotoxic response. In this study, the possibility of formation of three possible metabolites, given by the O-dealkylation of 3-OCH$_3$, 4-OCH$_3$ and 6-OCH$_3$ groups, can lead to liver damage at high doses administered and isolated from chalcones 1 and 2, where the inhibition effect of major species of CYP450 suggests an active principle based on the control of the administered oral dose.

Another structure-based prediction refers to the cardiotoxicity model, associated with the blockade of hERG (human Ether-a-go-go Related Gene) channels, a K$^+$ion transporter in the cardiovascular system. A structural database, which constitutes a test of similarity with cardiotoxic substructures, was able to quantify the degree of affinity of the chalcones towards this toxicity pathway, where it was possible to identify that the hydroxyl group constitutes, at the same time in

the two chalcones, a fragment capable of interacting with hERG channels. In contrast, the aromatic rings constitute positive fragments that decrease the channel inhibition potential.

5. Conclusion

The chalcones synthesized from the natural compound 2-hydroxy-3,4,6-trimethoxyacetophenone showed no toxicity under the conditions and doses evaluated here and showed anxiolytic effects. Thus, it was observed that the anxiolytic effects of chalcones **1** and **2** were antagonized by flumazenil, suggesting strong evidence of the involvement of GABA$_A$ receptors. Molecular docking results showed that chalcones have a higher affinity for the GABA$_A$ receptor than DZP and binding in the same region of the DZP binding site, indicating a similar effect to the drug. Chalcone *2* also had its anxiolytic action reversed by granisetron, which indicates that it acts through the participation of serotoninergic receptors 5HTR3A, which, according to molecular docking, binds to the transmembrane domain (TMD), a region different from the binding site of the granisetron inhibitor, co-crystallized in the extracellular domain (ECD), indicating a possible synergistic effect, since they do not compete for the same binding site. Therefore, substituents and their positions are relevant in studies of the structure-activity relationship. The interaction of chalcones with GABA$_A$ and 5-HT$_{3A}$ receptors demonstrates the pharmacological potential of these molecules and thus provides insights for the development of new drugs that act in the CNS.

Disclosure statement

No potential conflict of interest was reported by the authors.

ORCID

Francisco Rogênio Silva Mendes 🆔 http://orcid.org/0000-0001-8357-6707
Antonio Wlisses da Silva 🆔 http://orcid.org/0000-0002-1686-1644
Maria Kueirislene Amâncio Ferreira 🆔 http://orcid.org/0000-0002-4270-8109
Emanuela de Lima Rebouças 🆔 http://orcid.org/0000-0002-0572-5196
Italo Moura Barbosa 🆔 http://orcid.org/0000-0003-4621-7355
Matheus Nunes da Rocha 🆔 http://orcid.org/0000-0002-0929-4565

Ramon Róseo Paula Pessoa Bezerra de Menezes 🆔 http://orcid.org/0000-0003-3109-9683
Emanuel Paula Magalhães 🆔 http://orcid.org/0000-0002-8041-7935
Emanuelle Machado Marinho 🆔 http://orcid.org/0000-0003-1548-8574
Márcia Machado Marinho 🆔 http://orcid.org/0000-0002-7640-2220
Paulo Nogueira Bandeira 🆔 http://orcid.org/0000-0001-5374-1839
Jane Eire Silva Alencar de Menezes 🆔 http://orcid.org/0000-0001-9632-5464
Emmanuel Silva Marinho 🆔 http://orcid.org/0000-0002-4774-8775
Hélcio Silva dos Santos 🆔 http://orcid.org/0000-0001-5527-164X

References

Ahmad, F., & Richardson, M. K. (2013). Exploratory behaviour in the open field test adapted for larval zebrafish: Impact of environmental complexity. *Behavioural Processes*, *92*, 88–98. https://doi.org/10.1016/j.beproc.2012.10.014

Amali, M. O., Atunwa, S. A., Aiyelero, O. M., & Omotesho, Q. A. (2019). Assessment of anxiolytic potential and acute toxicity study of combretum micranthum g. don. leaves (combretaceae) in mice. *IBRO Reports*, *7*, 42. https://doi.org/10.1016/j.ibror.2019.09.085

Arellano-Aguiar, O., Solis-Angeles, S., Serrano-García, L., Morales-Sierra, E., Mendez-Serrano, A., Montero-Montoya, R. (2015). Use of the Zebrafish Embryo Toxicity Test for Risk Assessment Purpose: Case Study. *Fisheriessciences.com*, *9*(4), 052–062.

Arshia, A. H., Shadravan, S., Solhjoo, A., Sakhteman, A., & Sami, A. (2021). De novo design of novel protease inhibitor candidates in the treatment of SARS-CoV-2 using deep learning, docking, and molecular dynamic simulations. *Computers in Biology and Medicine*, *139*, 104967. https://doi.org/10.1016/j.compbiomed.2021.104967

Bai, Q., Tan, S., Xu, T., Liu, H., Huang, J., & Yao, X. (2021). MolAICal: a soft tool for 3D drug design of protein targets by artificial intelligence and classical algorithm. *Briefings in Bioinformatics*, *22*(3), 1–12. https://doi.org/10.1093/bib/bbaa161

Basak, S., Gicheru, Y., Kapoor, A., Mayer, M. L., Filizola, M., & Chakrapani, S. (2019). Molecular mechanism of setron-mediated inhibition of full-length 5-HT3A receptor. *Nature Communications*, *10*(1), 1–11. https://doi.org/10.1038/s41467-019-11142-8

Batista de Andrade Neto, J., Pessoa de Farias Cabral, V., Brito Nogueira, L. F., Rocha da Silva, C., Gurgel do Amaral Valente Sá, L., Ramos da Silva, A., Barbosa da Silva, W. M., Silva, J., Marinho, E. S., Cavalcanti, B. C., Odorico de Moraes, M., & Nobre Júnior, H. V. (2021). Anti-MRSA activity of curcumin in planktonic cells and biofilms and determination of possible action mechanisms. *Microbial Pathogenesis*, *155*, 104892. https://doi.org/10.1016/j.micpath.2021.104892

Benneh, C. K., Biney, R. P., Mante, P. K., Tandoh, A., Adongo, D. W., & Woode, E. (2017). Maerua angolensis stem bark extract reverses anxiety and related behaviours in zebrafish—Involvement of GABAergic and 5-HT systems. *Journal of Ethnopharmacology*, *207*, 129–145. https://doi.org/10.1016/j.jep.2017.06.012

Biovia, D. S. (2016). *Discovery studio modeling environment, release 2017, San Diego*. Dassault Systèmes.

Bugel, S. M., & Tanguay, R. L. (2018). Multidimensional chemobehavior analysis of flavonoids and neuroactive compounds in zebrafish. *Toxicology and Applied Pharmacology*, *344*(February), 23–34. https://doi.org/10.1016/j.taap.2018.02.019

Buxeraud, J., & Faure, S. (2019). Benzodiazepines. *Actualites Pharmaceutiques*, *58*(591), 24-26. https://doi.org/10.1016/j.actpha.2019.09.027

Cachat, J., Stewart, A., Utterback, E., Hart, P., Gaikwad, S., Wong, K., Kyzar, E., Wu, N., & Kalueff, A. V. (2011). Three-dimensional neurophenotyping of adult zebrafish behavior. *PLoS One*, *6*(3), e17597. https://doi.org/10.1371/journal.pone.0017597

Celada, P., Bortolozzi, A., & Artigas, F. (2013). Serotonin 5-HT1A receptors as targets for agents to treat psychiatric disorders: Rationale and current status of research. *CNS Drugs*, *27*(9), 703–716. https://doi.org/10.1007/s40263-013-0071-0

Chegini, H. R., Nasehi, M., & Zarrindast, M. R. (2014). Differential role of the basolateral amygdala 5-HT3 and 5-HT4 serotonin receptors upon

ACPA-induced anxiolytic-like behaviors and emotional memory deficit in mice. *Behavioural Brain Research*, 261, 114–126. https://doi.org/10.1016/j.bbr.2013.12.007

Chisholm, D., Sweeny, K., Sheehan, P., Rasmussen, B., Smit, F., Cuijpers, P., & Saxena, S. (2016). Scaling-up treatment of depression and anxiety: A global return on investment analysis. *The Lancet. Psychiatry*, 3(5), 415–424. https://doi.org/10.1016/S2215-0366(16)30024-4

Cho, S., Kim, S., Jin, Z., Yang, H., Han, D., Baek, N. I., Jo, J., Cho, C. W., Park, J. H., Shimizu, M., & Jin, Y. H. (2011). Isoliquiritigenin, a chalcone compound, is a positive allosteric modulator of GABA A receptors and shows hypnotic effects. *Biochemical and Biophysical Research Communications*, 413(4), 637–642. https://doi.org/10.1016/j.bbrc.2011.09.026

Cosacak, M. I., Bhattarai, P., Bocova, L., Dzewas, T., Mashkaryan, V., Papadimitriou, C., Brandt, K., Hollak, H., Antos, C. L., & Kizil, C. (2017). Human TAUP301L overexpression results in TAU hyperphosphorylation without neurofibrillary tangles in adult zebrafish brain. *Scientific Reports*, 7(1), 1–14. https://doi.org/10.1038/s41598-017-13311-5

Costall, B., & Naylor, R. J. (2004). 5- HT 3 Receptors. *Current Drug Targets. CNS and Neurological Disorders*, 3(1), 27–37. https://doi.org/10.1002/9780470015902.a0027709

Csizmadia, P. (2019). MarvinSketch and MarvinView: Molecule applets for the world wide web.*The 3rd International Electronic Conference on Synthetic Organic Chemistry*. https://doi.org/10.3390/ecsoc-3-01775

da Silva, A. W., Ferreira, M. K. A., Pereira, L. R., Rebouças, E. L., Coutinho, M. R., Dos, J., Lima, R., Guedes, M. I. F., Bandeira, P. N., Magalhães, F. E. A., Menezes, J. E. S. A. d., Marinho, M. M., Teixeira, A. M. R., Salles Trevisan, M. T., dos Santos, H. S., & Marinho, E. S. (2021). Combretum lanceolatum extract reverses anxiety and seizure behavior in adult zebrafish through GABAergic neurotransmission: an in vivo and in silico study. *Journal of Biomolecular Structure and Dynamics*, 40(20), 9801-9814.https://doi.org/10.1080/07391102.2021.1935322

da Silva, A. W., Ferreira, M. K. A., Rebouças, E. L., Mendes, F. R. S., Atilano, A. L., de Menezes, J. E. S. A., Marinho, M. M., Marinho, E. S., Santos, H. S., & Teixeira, A. M. R. (2021). Anxiolytic-like effect of natural product 2-hydroxy-3,4,6-trimethoxyacetophenone isolated from Croton anisodontus in adult zebrafish via serotonergic neuromodulation involvement of the 5-HT system. *Naunyn-Schmiedeberg's Archives of Pharmacology*, 394, 2023–2032. https://doi.org/10.1007/s00210-021-02116-z

da Silva, P. T., Lopes, L. M. A., Xavier, J. D. C., De Carvalho, M. C. S., De Moraes, M. O., Pessoa, C., Barros-Nepomuceno, F. W. A., Bandeira, P. N., Targino, C. S. D. P. C., Teixeira, A. M. R., Fontenelle, R. O. D. S., & Santos, H. S. (2020). Cytotoxic and antifungal activity of chalcones synthesized from natural acetophenone isolated from Croton anisodontus. *Revista Virtual De Química*, 12(3), 712–723. https://doi.org/10.21577/1984-6835.20200057

DasGupta, D., Mandalaparthy, V., & Jayaram, B. (2017). A component analysis of the free energies of folding of 35 proteins: A consensus view on the thermodynamics of folding at the molecular level. *Journal of Computational Chemistry*, 38(32), 2791–2801. https://doi.org/10.1002/jcc.25072

De Campos-Buzzi, F., Padaratz, P., Meira, A. V., Corrêa, R., Nunes, R. J., & Cechinel-Filho, V. (2007). 4′-Acetamidochalcone derivatives as potential antinociceptive agents. *Molecules*, 12(4), 896–906. https://doi.org/10.3390/12040896

DeLano, W. L. (2020). *The PyMOL molecular graphics system, Version 2.3.* Schrödinger LLC. https://doi.org/10.1038/hr.2014.17

Diaza, R. G., Manganelli, S., Esposito, A., Roncaglioni, A., Manganaro, A., & Benfenati, E. (2015). Comparison of in silico tools for evaluating rat oral acute toxicity. *SAR and QSAR in Environmental Research*, 26(1), 1–27. https://doi.org/10.1080/1062936X.2014.977819

Diez, M., Petuya, V., Martínez-Cruz, L. A., & Hernández, A. (2014). Insights into mechanism kinematics for protein motion simulation. *BMC Bioinformatics*, 15(1), 184. https://doi.org/10.1186/1471-2105-15-184

Farago, O. (2019). Langevin thermostat for robust configurational and kinetic sampling. *Physica A: Statistical Mechanics and Its Applications*, 534(122210), 122210. https://doi.org/10.1016/j.physa.2019.122210

Ferreira, M. K. A., da Silva, A. W., dos Santos Moura, A. L., Sales, K. V. B., Marinho, E. M., do Nascimento Martins Cardoso, J., Marinho, M. M.,

Bandeira, P. N., Magalhães, F. E. A., Marinho, E. S., de Menezes, J. E. S. A., & dos Santos, H. S. (2021). Chalcones reverse the anxiety and convulsive behavior of adult zebrafish. *Epilepsy & Behavior: E&B*, 117, 107881. https://doi.org/10.1016/j.yebeh.2021.107881

Ferreira, M. K. A., da Silva, A. W., Silva, F. C. O., Holanda, C. L. A., Barroso, S. M., Lima, J., dos, R., Vieira Neto, A. E., Campos, A. R., Bandeira, P. N., dos Santos, H. S., de Lemos, T. L. G., Siqueira, S. M. C., Magalhães, F. E. A., & de Menezes, J. E. S. A. (2019). Anxiolytic-like effect of chalcone N-{(4'-[(E)-3-(4-fluorophenyl)-1-(phenyl) prop-2-en-1-one]} acetamide on adult zebrafish (Danio rerio): Involvement of the GABAergic system. *Behavioural Brain Research*, 374, 111871. https://doi.org/10.1016/j.bbr.2019.03.040

Ferreira, M. K. A., da Silva, A. W., Silva, F. C. O., Vieira Neto, A. E., Campos, A. R., Alves Rodrigues Santos, S. A., Rodrigues Teixeira, A. M., da Cunha Xavier, J., Bandeira, P. N., Sampaio Nogueira, C. E., de Brito, D. H. A., Rebouças, E. L., Magalhães, F. E. A., de Menezes, J. E. S. A., & dos Santos, H. S. (2020). Anxiolytic-like effect of chalcone N-{4′[(2E)-3-(3-nitrophenyl)-1-(phenyl)prop-2-en-1-one]} acetamide on adult zebrafish (Danio rerio): Involvement of the 5-HT system. *Biochemical and Biophysical Research Communications*, 526(2), 505–511. https://doi.org/10.1016/j.bbrc.2020.03.129

Gebauer, D. L., Pagnussat, N., Piato, Â. L., Schaefer, I. C., Bonan, C. D., & Lara, D. R. (2011). Effects of anxiolytics in zebrafish: Similarities and differences between benzodiazepines, buspirone and ethanol. *Pharmacology, Biochemistry, and Behavior*, 99(3), 480–486. https://doi.org/10.1016/j.pbb.2011.04.021

Gleeson, M. P. (2008). Generation of a set of simple, interpretable ADMET rules of thumb. *Journal of Medicinal Chemistry*, 51(4), 817–834. https://doi.org/10.1021/jm701122q

Gohlke, H., & Case, D. A. (2004). Converging free energy estimates: MM-PB(GB)SA studies on the protein-protein complex Ras-Raf. *Journal of Computational Chemistry*, 25(2), 238–250. https://doi.org/10.1002/jcc.10379

Gohlke, H., Kiel, C., & Case, D. A. (2003). Insights into protein-protein binding by binding free energy calculation and free energy decomposition for the Ras-Raf and Ras-RalGDS complexes. *Journal of Molecular Biology*, 330(4), 891–913. https://doi.org/10.1016/S0022-2836(03)00610-7

Golani, L. K., Yeunus Mian, M., Ahmed, T., Pandey, K. P., Mondal, P., Sharmin, D., Rezvanian, S., Witkin, J. M., & Cook, J. M. (2022). Rationalizing the binding and α subtype selectivity of synthesized imidazodiazepines and benzodiazepines at GABAA receptors by using molecular docking studies. *Bioorganic & Medicinal Chemistry Letters*, 62(July 2021), 128637. https://doi.org/10.1016/j.bmcl.2022.128637

Gonçalves, N. G. G., de Araújo, J. I. F., Magalhães, F. E. A., Mendes, F. R. S., Lobo, M. D. P., Moreira, A. C. d. O. M., Moreira, R., & de, A. (2020). Protein fraction from Artocarpus altilis pulp exhibits antioxidant properties and reverses anxiety behavior in adult zebrafish via the serotoninergic system. *Journal of Functional Foods*, 66(April 2019), 103772. https://doi.org/10.1016/j.jff.2019.103772

Gupta, P., Khobragade, S., Rajaram, S., & Shingatgeri, V. (2014). Assessment of locomotion behavior in adult Zebrafish after acute exposure to different pharmacological reference compounds. *Drug Development and Therapeutics*, 5(2), 127. https://doi.org/10.4103/2394-2002.139626

Halgren, T. A. (1996). Merck molecular force field. I. Basis, form, scope, parameterization, and performance of MMFF94. *Journal of Computational Chemistry*, 17(5-6), 490–519. https://doi.org/10.1002/(SICI)1096-987X(199604)17:5/6 < 490::AID-JCC1 > 3.0.CO;2-P

Hanson, D. R., & Gottesman, I. I. (2012). Biologically flavored perspectives on Garmezian resilience. *Development and Psychopathology*, 24(2), 363–369. https://doi.org/10.1017/S0954579412000041

Hanwell, M. D., Curtis, D. E., Lonie, D. C., Vandermeersch, T., Zurek, E., & Hutchison, G. R. (2012). Avogadro: an advanced semantic chemical editor, visualization, and analysis platform. *Journal of Cheminformatics*, 4(1), 17. https://doi.org/10.1186/1758-2946-4-17

Higgs, J., Wasowski, C., Marcos, A., Jukič, M., Paván, C. H., Gobec, S., de Tezanos Pinto, F., Colettis, N., & Marder, M. (2019). Chalcone derivatives: synthesis, in vitro and in vivo evaluation of their anti-anxiety,

anti-depression and analgesic effects. *Heliyon*, *5*(3), e01376. https://doi.org/10.1016/j.heliyon.2019.e01376

Hood, S., O'Neil, G., & Hulse, G. (2009). The role of flumazenil in the treatment of benzodiazepine dependence: Physiological and psychological profiles. *Journal of Psychopharmacology (Oxford, England)*, *23*(4), 401–409. https://doi.org/10.1177/0269881108100322

Huey, R., Morris, G. M., & Forli, S. (2012). Using AutoDock 4 and AutoDock Vina with AutoDockTools: A tutorial. *The Scripps Research Institute Molecular*, 2-28.

Hughes, J. D., Blagg, J., Price, D. A., Bailey, S., DeCrescenzo, G. A., Devraj, R. V., Ellsworth, E., Fobian, Y. M., Gibbs, M. E., Gilles, R. W., Greene, N., Huang, E., Krieger-Burke, T., Loesel, J., Wager, T., Whiteley, L., & Zhang, Y. (2008). Physiochemical drug properties associated with in vivo toxicological outcomes. *Bioorganic & Medicinal Chemistry Letters*, *18*(17), 4872–4875. https://doi.org/10.1016/j.bmcl.2008.07.071

Humphrey, W., Dalke, A., & Schulten, K. (1996). VMD: Visual molecular dynamics. *Journal of Molecular Graphics*, *14*(1), 33–38. https://doi.org/10.1016/0263-7855(96)00018-5

Johnson, T. W., Dress, K. R., & Edwards, M. (2009). Using the Golden Triangle to optimize clearance and oral absorption. *Bioorganic & Medicinal Chemistry Letters*, *19*(19), 5560–5564. https://doi.org/10.1016/j.bmcl.2009.08.045

Kato, K., Nakayoshi, T., Kurimoto, E., & Oda, A. (2021). Molecular dynamics simulations for the protein–ligand complex structures obtained by computational docking studies using implicit or explicit solvents. *Chemical Physics Letters*, *781*(139022), 139022. https://doi.org/10.1016/j.cplett.2021.139022

Lima, A. H., Souza, P. R. M., Alencar, N., Lameira, J., Govender, T., Kruger, H. G., Maguire, G. E. M., & Alves, C. N. (2012). Molecular Modeling of T. rangeli, T. brucei gambiense, and T. evansi sialidases in complex with the DANA Inhibitor. *Chemical Biology & Drug Design*, *80*(1), 114–120. https://doi.org/10.1111/j.1747-0285.2012.01380.x

Lipinski, C. A. (2004). Lead- and drug-like compounds: The rule-of-five revolution. *Drug Discovery Today. Technologies*, *1*(4), 337–341. https://doi.org/10.1016/j.ddtec.2004.11.007

Marder, M. (2012). Flavonoids as GABAA receptor ligands: the whole story? *Journal of Experimental Pharmacology*, *4*, 9–24. https://doi.org/10.2147/jep.s23105

Marinho, E. M., Batista de Andrade Neto, J., Silva, J., Rocha da Silva, C., Cavalcanti, B. C., Marinho, E. S., & Nobre Júnior, H. V. (2020). Virtual screening based on molecular docking of possible inhibitors of Covid-19 main protease. *Microbial Pathogenesis*, *148*, 104365. https://doi.org/10.1016/j.micpath.2020.104365

Masiulis, S., Desai, R., Uchański, T., Serna Martin, I., Laverty, D., Karia, D., Malinauskas, T., Zivanov, J., Pardon, E., Kotecha, A., Steyaert, J., Miller, K. W., & Aricescu, A. R. (2019). GABAA receptor signalling mechanisms revealed by structural pharmacology. *Nature*, *565*(7740), 454–459. https://doi.org/10.1038/s41586-018-0832-5

Maximino, C., de Brito, T. M., Colmanetti, R., Pontes, A. A. A., de Castro, H. M., de Lacerda, R. I. T., Morato, S., & Gouveia, A. (2010). Parametric analyses of anxiety in zebrafish scototaxis. *Behavioural Brain Research*, *210*(1), 1–7. https://doi.org/10.1016/j.bbr.2010.01.031

Oliveira, D. R. d., Todo, A. H., Rêgo, G. M., Cerutti, J. M., Cavalheiro, A. J., Rando, D. G. G., & Cerutti, S. M. (2018). Flavones-bound in benzodiazepine site on GABAA receptor: Concomitant anxiolytic-like and cognitive-enhancing effects produced by Isovitexin and 6-C-glycoside-Diosmetin. *European Journal of Pharmacology*, *831*(April), 77–86. https://doi.org/10.1016/j.ejphar.2018.05.004

Morris, G. M., Huey R Fau- Lindstrom, W., Lindstrom W Fau- Sanner, M. F., Sanner Mf Fau- Belew, R. K., Belew Rk Fau- Goodsell, D. S., Goodsell Ds Fau- Olson, A. J., Olson, A. J., & Chem, J. C. (2009). AutoDock4 and AutoDockTools4: Automated docking with selective receptor flexibility. *Journal of Computational Chemistry*, *30*(16), 2785–2791.

Mosmann, T. (1983). Rapid colorimetric assay for cellular growth and survival: Application to proliferation and cytotoxicity assays. *Journal of Immunological Methods*, *65*(1-2), 55–63. https://doi.org/10.1016/0022-1759(83)90303-4

Olivier, B., Wijngaarden, I. V., & Soudijn, W. (2000). 5-HT3 receptor antagonists and anxiety; A preclinical and clinical review. *European Neuropsychopharmacology: The Journal of the European College of Neuropsychopharmacology*, *10*(2), 77–95. https://doi.org/10.1016/S0924-977X(99)00065-6

Pettersen, E. F., Goddard, T. D., Huang, C. C., Couch, G. S., Greenblatt, D. M., Meng, E. C., & Ferrin, T. E. (2004). UCSF Chimera - A visualization system for exploratory research and analysis. *Journal of Computational Chemistry*, *25*(13), 1605–1612. https://doi.org/10.1002/jcc.20084

Phillips, J. C., Braun, R., Wang, W., Gumbart, J., Tajkhorshid, E., Villa, E., Chipot, C., Skeel, R. D., Kalé, L., & Schulten, K. (2005). Scalable molecular dynamics with NAMD. *Journal of Computational Chemistry*, *26*(16), 1781–1802. https://doi.org/10.1002/jcc.20289

Rajkumar, R., & Mahesh, R. (2010). The auspicious role of the 5-HT3 receptor in depression: A probable neuronal target? *Journal of Psychopharmacology (Oxford, England)*, *24*(4), 455–469. https://doi.org/10.1177/0269881109348161

Rani, A., Singh, A., Kaur, J., Singh, G., Bhatti, R., Gumede, N., Kisten, P., Singh, P., Kumar., & V., Sumanjit. (2021). 1H-1,2,3-triazole grafted tacrine-chalcone conjugates as potential cholinesterase inhibitors with the evaluation of their behavioral tests and oxidative stress in mice brain cells. *Bioorganic Chemistry*, *114*(September 2020), 105053. https://doi.org/10.1016/j.bioorg.2021.105053

Rojas, J., Domínguez, J. N., Charris, J. E., Lobo, G., Payá, M., & Ferrándiz, M. L. (2002). Synthesis and inhibitory activity of dimethylamino-chalcone derivatives on the induction of nitric oxide synthase. *European Journal of Medicinal Chemistry*, *37*(8), 699–705. https://doi.org/10.1016/s0223-5234(02)01387-9

Rose, A. S., Bradley, A. R., Valasatava, Y., Duarte, J. M., Prlic, A., & Rose, P. W. (2018). NGL viewer: Web-based molecular graphics for large complexes. *Bioinformatics (Oxford, England)*, *34*(21), 3755–3758. https://doi.org/10.1093/bioinformatics/bty419

Salehi, B., Quispe, C., Chamkhi, I., El Omari, N., Balahbib, A., Sharifi-Rad, J., Bouyahya, A., Akram, M., Iqbal, M., Docea, A. O., Caruntu, C., Leyva-Gómez, G., Dey, A., Martorell, M., Calina, D., López, V., & Les, F. (2021). Pharmacological properties of chalcones: A review of preclinical including molecular mechanisms and clinical evidence. *Frontiers in Pharmacology*, *11*, 1-21. https://doi.org/10.3389/fphar.2020.592654

Shityakov, S., & Foerster, C. (2014). In silico predictive model to determine vector-mediated transport properties for the blood-brain barrier choline transporter. *Advances and Applications in Bioinformatics and Chemistry*, *2014*(7), 23-36. https://doi.org/10.2147/AABC.S63749

Silva Mendes, F. R., Wlisses da Silva, A., Amâncio Ferreira, M. K., de Lima Rebouças, E., Marinho, E. M., Marinho, M. M., Bandeira, P. N., Rodrigues Teixeira, A. M., Silva Alencar de Menezes, J. E., Alves de Siqueira, E., Róseo Paula Pessoa Bezerra de Menezes, R., Marinho, E. S., & Silva dos Santos, H. (2022). GABAA receptor participation in anxiolytic and anticonvulsant effects of (E)-3-(furan-2-yl)-1-(2hydroxy-3,4,6-trimethoxyphenyl)prop-2-en-1-one in adult zebrafish. *Neurochemistry International*, *155*(October 2021), 105303. https://doi.org/10.1016/j.neuint.2022.105303

Silva, J., Rocha, M. N. d., Marinho, E. M., Marinho, M. M., Marinho, E. S., & Santos, H. S. d (2021). Evaluation of the ADME, toxicological analysis and molecular docking studies of the anacardic acid derivatives with potential antibacterial effects against Staphylococcus aureus. *Journal of Analytical & Pharmaceutical Research*, *10*(5), 177–194. https://doi.org/10.15406/japlr.2021.10.00384

Stewart, A. M., Braubach, O., Spitsbergen, J., Gerlai, R., & Kalueff, A. V. (2014). Zebrafish models for translational neuroscience research: From tank to bedside. *Trends in Neurosciences*, *37*(5), 264–278. https://doi.org/10.1016/j.tins.2014.02.011

Stewart, A., Gaikwad, S., Kyzar, E., Green, J., Roth, A., & Kalueff, A. V. (2012). Modeling anxiety using adult zebrafish: A conceptual review. *Neuropharmacology*, *62*(1), 135–143. https://doi.org/10.1016/j.neuropharm.2011.07.037

Stewart, A., Wu, N., Cachat, J., Hart, P., Gaikwad, S., Wong, K., Utterback, E., Gilder, T., Kyzar, E., Newman, A., Carlos, D., Chang, K., Hook, M., Rhymes, C., Caffery, M., Greenberg, M., Zadina, J., & Kalueff, A. V. (2011). Pharmacological modulation of anxiety-like phenotypes in adult zebrafish behavioral models. *Progress in Neuro-Psychopharmacology & Biological Psychiatry*, *35*(6), 1421–1431. https://doi.org/10.1016/j.pnpbp.2010.11.035

Trott, O., & Olson, A. J. (2010). AutoDock Vina: improving the speed and accuracy of docking with a new scoring function, efficient optimization, and multithreading. *Journal of Computational Chemistry*, *31*(2), 455–461. https://doi.org/10.1002/jcc.21334

Vos, T., Lim, S. S., Abbafati, C., Abbas, K. M., Abbasi, M., Abbasifard, M., Abbasi-Kangevari, M., Abbastabar, H., Abd-Allah, F., Abdelalim, A., Abdollahi, M., Abdollahpour, I., Abolhassani, H., Aboyans, V., Abrams, E. M., Abreu, L. G., Abrigo, M. R. M., Abu-Raddad, L. J., Abushouk, A. I., … Murray, C. J. L. (2020). Global burden of 369 diseases and injuries in 204 countries and territories, 1990–2019: a systematic analysis for the Global Burden of Disease Study 2019. *The Lancet*, *396*(10258), 1204–1222. https://doi.org/10.1016/S0140-6736(20)30925-9

Wiatrak, B., Kubis-Kubiak, A., Piwowar, A., & Barg, E. (2020). PC12 Cell Line: Cell types, coating of culture vessels, differentiation and other culture conditions. *Cells*, *9*(4), 958. https://doi.org/10.3390/cells9040958

World Health Organization. (2017). *Depression and other common mental disorders*. Global Health Estimates.

Yan, J., Zhang, G., Pan, J., & Wang, Y. (2014). α-Glucosidase inhibition by luteolin: Kinetics, interaction and molecular docking. *International Journal of Biological Macromolecules*, *64*, 213–223. https://doi.org/10.1016/j.ijbiomac.2013.12.007

Yusuf, D., Davis, A. M., Kleywegt, G. J., & Schmitt, S. (2008). An alternative method for the evaluation of docking performance: RSR vs RMSD. *Journal of Chemical Information and Modeling*, *48*(7), 1411–1422. https://doi.org/10.1021/ci800084x